nature communications

Article

https://doi.org/10.1038/s41467-025-65573-7

GPR43 in eosinophils suppresses the emergence of pathogenic Siglec-F^{hi} neutrophils in allergic airway inflammation in mice

Received: 4 September 2024

Accepted: 18 October 2025

Published online: 26 November 2025

Check for updates

Jihyun Yu[1], Seongryong Kim[1], Hyun-Sup Song[1], Jieun Kim[2], Woojung Shin[2], Jong-Eun Park[1], Ikuo Kimura[3], Hye-Young Kim[4] & You-Me Kim[1]

Eosinophils are major effector cells in type 2 immune responses, contributing to host defense and allergic diseases. They also contribute to maintaining tissue homeostasis by regulating various immune cell types, including neutrophils. Here we show that eosinophils directly associate with neutrophils in the lungs of asthma-induced mice. Eosinophil-specific deficiency of the short-chain fatty acid receptor, GPR43, results in hyperactivation of eosinophils and increases the expression of neutrophil chemoattractants and PECAM-1, thereby enhancing the interaction between eosinophils and neutrophils. This interaction exposes neutrophils to eosinophil-derived IL-4 and GM-CSF, which induce the conversion of conventional neutrophils into more pathogenic, Siglec-F^{hi} neutrophils capable of enhancing Th17 cell differentiation and aggravating asthma symptoms in mouse models. Our results thus implicate GPR43 as a critical regulator of eosinophils, and describe eosinophil-mediated modulation of neutrophil differentiation and function.

Eosinophils are multifunctional granulocytes that are primarily recruited during type 2 immune responses. Once activated, they degranulate and release pre-synthesized cationic proteins, cytokines, chemokines, and lipid mediators to protect the host from infectious agents. However, this potent response can also cause tissue damage in allergic diseases[1–3]. Moreover, eosinophils are constitutively present in several peripheral organs, where they maintain tissue homeostasis[4,5]. For example, eosinophils in adipose tissue are the major source of IL-4, which sustains the alternatively activated macrophages that control glucose metabolism[6]. Intestinal eosinophils not only dominate the myeloid cells in the gastrointestinal tract but also prevent inflammation by suppressing Th1 and Th17 cells[7,8]. In addition, eosinophils in the lung protect it from allergen-induced airway inflammation by suppressing dendritic cells (DCs)[9]. Notably, these local eosinophils markedly differ from newly infiltrating inflammatory eosinophils in terms of morphology and functions[9]. Thus, eosinophils have diverse functions and make complex interactions with other immune cell types.

The development, migration, and activation of eosinophils are regulated by common β chain cytokines, such as IL-3, IL-5, and GM-CSF[1,10]. In addition, recent studies suggest that tissue environmental factors and nutrient-derived signals can control eosinophil functions. For example, aryl hydrocarbon receptor signaling in intestinal eosinophils induces transcriptional programming that permits their adaptation to the local environment, extends their life span, and confers their unique characteristics[11,12]. Similarly, the programming of intestinal eosinophils is also driven directly by retinoic acid: this signaling is specifically required for maintaining a villus-resident subpopulation of intestinal eosinophils[13]. Moreover, the binding of neuromedin-U, a neuropeptide produced in the gut, to its receptor on

[1]Graduate School of Medical Science and Engineering, Korea Advanced Institute of Science and Technology, Daejeon, Republic of Korea. [2]Department of Bio and Brain Engineering, Korea Advanced Institute of Science and Technology, Daejeon, Republic of Korea. [3]Graduate School of Biostudies, Kyoto University, Kyoto, Japan. [4]Department of Biomedical Sciences, Seoul National University College of Medicine, Seoul, Republic of Korea. e-mail: youmekim@kaist.ac.kr

eosinophils promotes their intestinal accumulation under normal conditions and induces goblet cell differentiation during helminth infection[14].

An interesting nutrient-derived factor is short-chain fatty acids (SCFAs), which are mainly produced by the gut microbiota via dietary fiber fermentation and circulated throughout the body[15–17]. SCFAs are recognized by GPR43, which is expressed by many non-immune and immune cells, including eosinophils[18,19]. Significantly, numerous studies show that SCFAs exert anti-inflammatory effects, and the lack of GPR43 signaling aggravates inflammatory diseases such as food allergy, colitis, rheumatoid arthritis, and asthma[18,20,21]. Various GPR43-bearing cells have been found to mediate this anti-inflammatory activity, including DCs, neutrophils, type 3 innate lymphoid cells, and intestinal epithelial cells[18,20–23]. However, whether eosinophils also have GPR43-mediated anti-inflammatory activities is unknown.

Here, we show with mice lacking GPR43 in eosinophils that GPR43 prevents eosinophils from becoming hyperactivated in allergic airway inflammation. Interestingly, this reduces direct eosinophil interactions with neutrophils in the lung, thereby suppressing the emergence of a pathogenic, Th17-promoting neutrophil subset. Thus, this study shows that GPR43 regulates eosinophil functions, and that eosinophils have a previously little-known ability to directly modulate neutrophil differentiation and activities in lung inflammation.

Results

GPR43 deficiency in eosinophils exacerbates asthma in association with increased lung neutrophils and Th17 cells

GPR43 is encoded by free fatty acid receptor 2 *(FFAR2)*. As previously observed[14,24–28], *FFAR2* is constitutively expressed at high levels in eosinophils from various organs in humans and mice. By contrast, other *FFAR* genes (*FFAR1* and *FFAR3*) are poorly expressed (Supplementary Fig. 1a, b). *Ffar2* is also expressed in eosinophils in the lungs of mice in which asthma was induced with house dust mite extracts (HDM) (Supplementary Fig. 1c). Moreover, publicly available single-cell RNA-sequencing (scRNA-seq) data from patients with eosinophilic esophagitis show that eosinophils in the inflamed esophagus and duodenum highly express *FFAR2*[29](Supplementary Fig. 1d, e). Given that GPR43 has well-known anti-inflammatory functions and eosinophils drive airway inflammation in asthma, we asked whether GPR43 regulates eosinophils in asthma.

To address this, GPR43 was specifically deleted in eosinophils by crossing *Gpr43*$^{fl/fl}$ mice with *Epx-Cre* mice, thus generating *Epx*$^{Cre/+}$*Gpr43*$^{fl/fl}$ mice. Eosinophil-specific Cre-mediated recombination was confirmed with *Epx*$^{Cre/+}$Rosa26-eYFP$^{fl/+}$ reporter mice. As reported previously[7], YFP was exclusively expressed in eosinophils, of which 60-70% expressed YFP (Supplementary Fig. 1f–h, 15). Notably, despite the apparently incomplete recombination induced by *Epx-Cre* in the reporter mice, GPR43 mRNA was not detected in eosinophils from *Epx*$^{Cre/+}$*Gpr43*$^{fl/fl}$ mice (Supplementary Fig. 1i). Moreover, acetate, an endogenous GPR43 ligand, did not induce Ca^{2+} influx in eosinophils from *Epx*$^{Cre/+}$*Gpr43*$^{fl/fl}$ mice (Supplementary Fig. 1j). Thus, GPR43 signaling is efficiently abrogated in GPR43-deficient eosinophils.

Epx$^{Cre/+}$*Gpr43*$^{fl/fl}$ and control (*Epx*$^{Cre/+}$) mice were then subjected to allergic airway inflammation induced by house dust mite extracts (Fig. 1a). To minimize variability arising from hormonal fluctuations, all experiments were initially conducted using male mice. Compared to *Epx*$^{Cre/+}$ mice, *Epx*$^{Cre/+}$*Gpr43*$^{fl/fl}$ mice had significantly more immune cells, including eosinophils and neutrophils, in the bronchoalveolar space (Fig. 1b and Supplementary Fig. 16a). Histological analysis revealed more inflammation, mucus accumulation, and fibrosis in the lungs of *Epx*$^{Cre/+}$*Gpr43*$^{fl/fl}$ mice (Fig. 1c). Accordingly, *Epx*$^{Cre/+}$*Gpr43*$^{fl/fl}$ mice showed worse airway hyperresponsiveness compared to control mice (Fig. 1d). Thus, GPR43 deletion in eosinophils aggravated airway inflammation and asthma symptoms. The bronchoalveolar

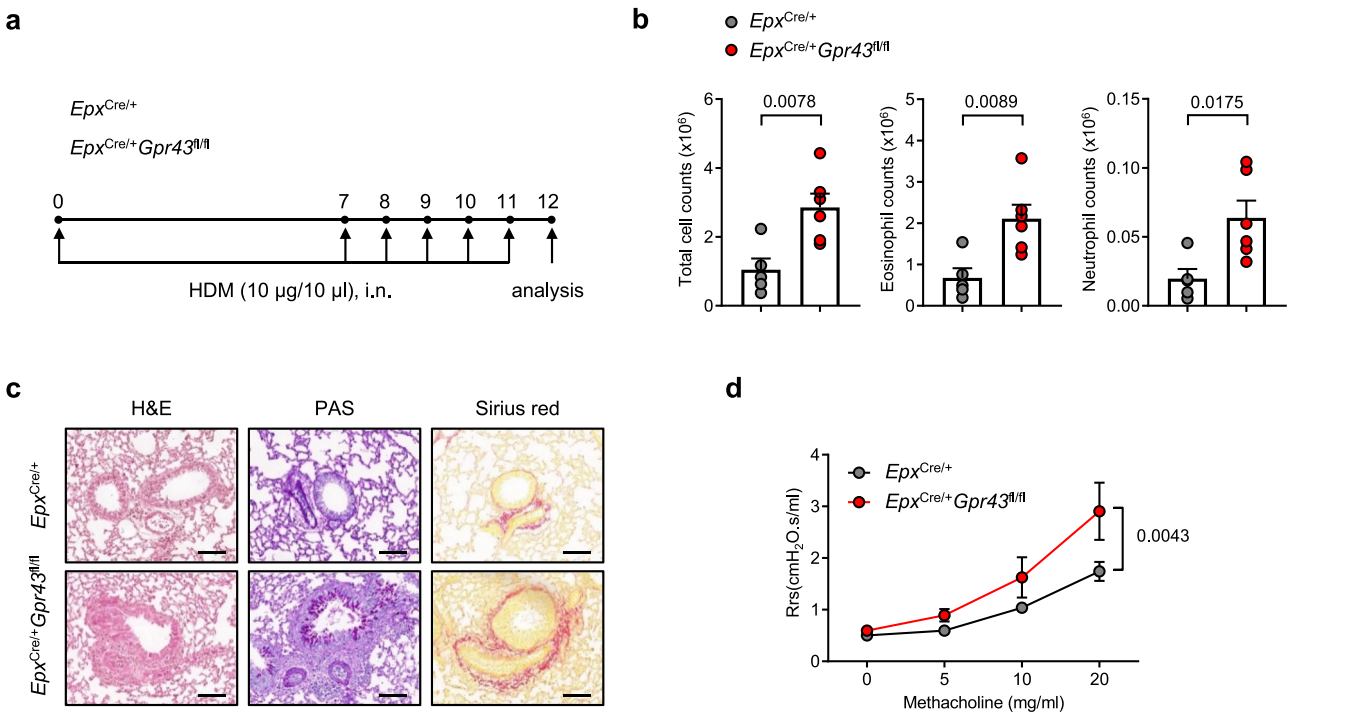

Fig. 1 | GPR43 deficiency in eosinophils exacerbates HDM-induced asthma. **a** Experimental scheme of HDM-induced asthma. **b** Total immune cell, eosinophil, and neutrophil counts in BALF. *Epx*$^{Cre/+}$ ($n = 5$), *Epx*$^{Cre/+}$*Gpr43*$^{fl/fl}$ ($n = 6$). Data are representative of more than three independent experiments. **c** Histological analysis of immune cell infiltration (H&E), mucus production (PAS), and fibrosis (Sirius red) in asthmatic lungs. Scale bar, 100 µm. Data are representative of two independent experiments. **d** Airway resistance. *Epx*$^{Cre/+}$ ($n = 9$), *Epx*$^{Cre/+}$*Gpr43*$^{fl/fl}$ ($n = 9$). Data pooled from two independent experiments. Data are presented as mean ± s.e.m. Statistical analysis was performed using an unpaired two-tailed Student's t-test (**b**) or two-way ANOVA (**d**).

https://doi.org/10.1038/s41467-025-65573-7

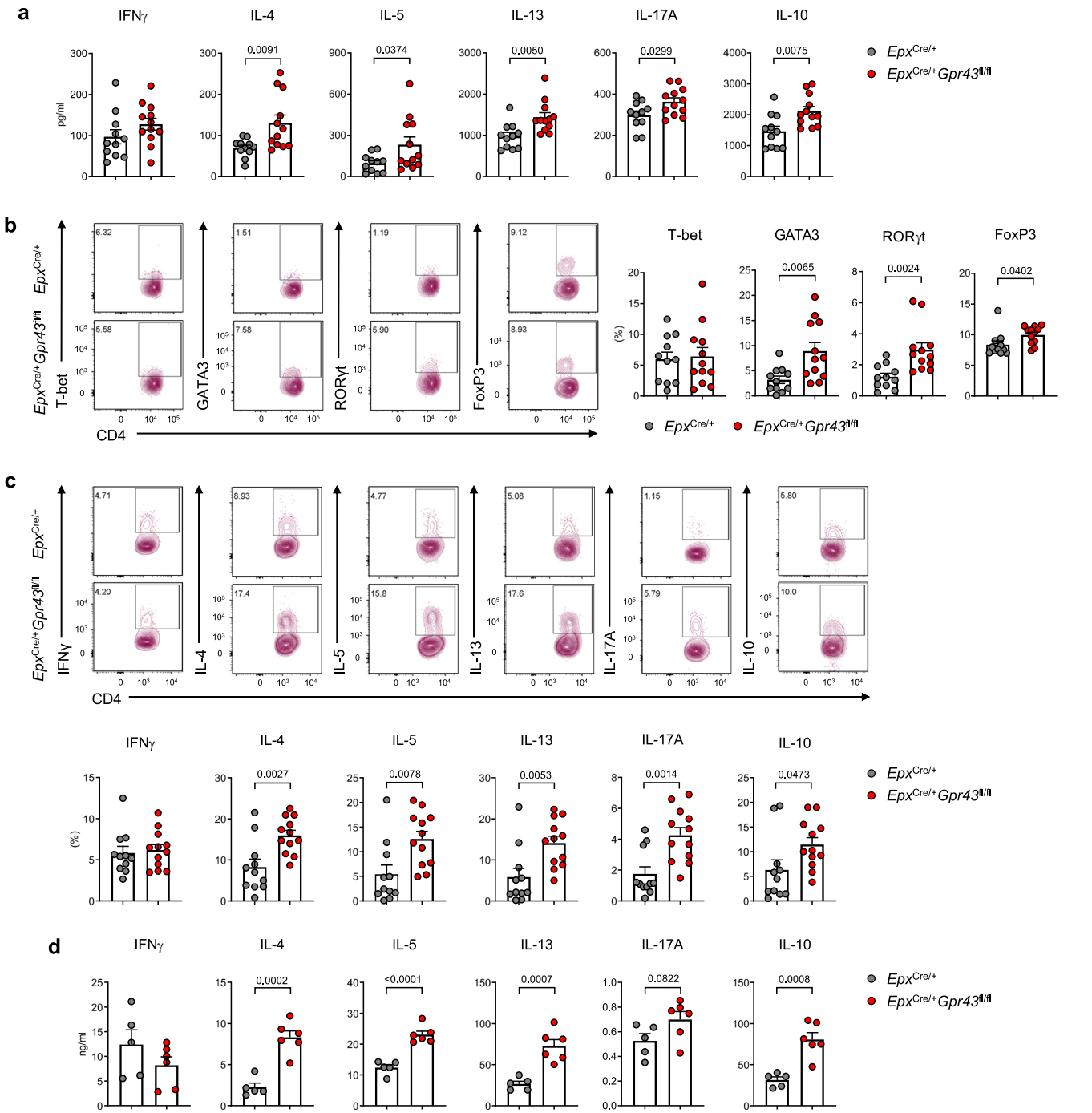

Fig. 2 | GPR43 deficiency in eosinophils upregulates Th2 and Th17 responses in HDM-induced asthma. a Cytokine levels in BALF. **b** Percentages of CD4 T cells expressing each transcription factor in asthmatic lungs. **c** Percentages of CD4 T cells producing each cytokine in asthmatic lungs. $Epx^{Cre/+}$ ($n = 11$), $Epx^{Cre/+}Gpr43^{fl/fl}$ ($n = 12$). Data in (**a**–**c**) were pooled from two independent experiments. **d** Cytokine levels in culture supernatants of asthmatic lung cells stimulated with anti-CD3 and anti-CD28. $Epx^{Cre/+}$ ($n = 5$), $Epx^{Cre/+}Gpr43^{fl/fl}$ ($n = 6$). Data in (**d**) are representative of three independent experiments. Data are presented as mean ± s.e.m. Statistical analysis was performed using an unpaired two-tailed Student's t-test.

lavage fluid (BALF) from asthmatic $Epx^{Cre/+}Gpr43^{fl/fl}$ mice also contained higher type 2 cytokine levels (IL-4, IL-5, and IL-13) (Fig. 2a) and their lungs bore more GATA3- and type 2 cytokine-expressing CD4 T cells (Fig. 2b–d and Supplementary Fig. 16b–d). Notably, the BALF from $Epx^{Cre/+}Gpr43^{fl/fl}$ mice also contained significantly more IL-17A, and the lungs bore higher frequencies of RORγt- and IL-17A-expressing CD4 T cells (Fig. 2a–d). These results show that GPR43 deficiency in eosinophils enhances both Th2 and Th17 immune responses in asthma.

Pathogenic Siglec-F^{hi} neutrophils accumulate in the asthmatic lungs of $Epx^{Cre/+}Gpr43^{fl/fl}$ mice

To comprehensively examine the effect of eosinophil-specific GPR43 deletion on the lung immune cell landscape during airway inflammation, CD45$^+$ cells from HDM-induced asthmatic lungs of $Epx^{Cre/+}$ and $Epx^{Cre/+}Gpr43^{fl/fl}$ mice were subjected to scRNA-seq. Unsupervised cell clustering revealed nine groups bearing conventional immune cell type markers (Fig. 3a and Supplementary Fig. 2a). Notably, eosinophils were not detected. This was also observed in publicly available scRNA-

https://doi.org/10.1038/s41467-025-65573-7

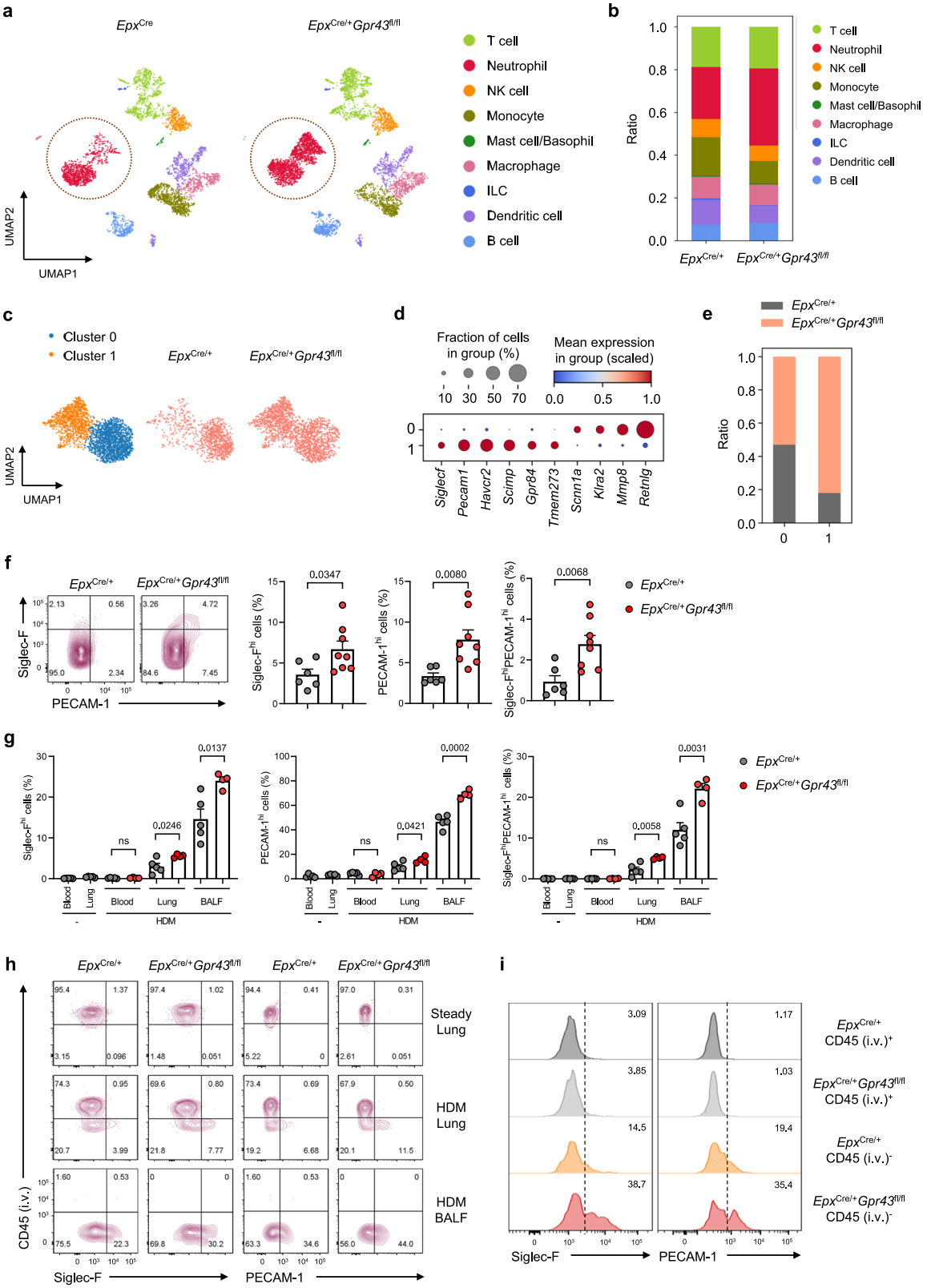

seq datasets of healthy and asthmatic lung[30,31] and probably reflects high RNase levels in eosinophils[30–32]. The most notable difference between *Epx*$^{Cre/+}$ and *Epx*$^{Cre/+}$*Gpr43*$^{fl/fl}$ mice was the neutrophils: they were highly enriched in *Epx*$^{Cre/+}$*Gpr43*$^{fl/fl}$ mice (Fig. 3b). Fine clustering of T cells showed that GPR43 deletion in eosinophils increased *Gata3*-, *Il4*-, *Il5*-, and *Il13*-expressing Th2 cells and *Rorc*- and *Il17*-expressing Th17 cells (Supplementary Fig. 2b–d). These findings are consistent with our flow cytometry results (Fig. 2b, c), despite the lack of statistical analysis in this transcriptomic data.

Subclustering of all neutrophils in our scRNA-seq datasets resulted in two distinct clusters (Fig. 3a, c). Both expressed *Cxcr2* and *S100a8* but other genes typically associated with neutrophils (e.g. *Mmp8* and *Retnlg*) demonstrated dramatic downregulation in Cluster 1. Moreover, several other genes were almost exclusively expressed in

Fig. 3 | Absence of GPR43 in eosinophils results in the emergence of pathogenic Siglec-F^{hi} neutrophils in asthmatic lungs. a–e CD45^{+} cells from three mice were pooled per group and subjected to single-cell RNA sequencing. UMAP plots of immune cells in asthmatic lungs of *Epx*$^{Cre/+}$ and *Epx*$^{Cre/+}$*Gpr43*$^{fl/fl}$ mice (**a**). Ratio of the immune cell types in each group (**b**). UMAP plots of neutrophils showing two distinct clusters (**c**). Dot plot of marker genes for each neutrophil cluster (**d**). Ratios of each group in the individual neutrophil clusters (**e**). **f** Percentages of Siglec-F^{hi}, PECAM-1^{hi}, and Siglec-F^{hi}PECAM-1^{hi} cells among neutrophils in asthmatic lungs. *Epx*$^{Cre/+}$ ($n = 6$), *Epx*$^{Cre/+}$*Gpr43*$^{fl/fl}$ ($n = 8$). **g** Percentages of Siglec-F^{hi}, PECAM-1^{hi}, and Siglec-F^{hi}PECAM-1^{hi} cells among neutrophils in blood, lung, and BALF. Steady-state *Epx*$^{Cre/+}$ ($n = 5$), asthmatic *Epx*$^{Cre/+}$ ($n = 5$), asthmatic *Epx*$^{Cre/+}$*Gpr43*$^{fl/fl}$ ($n = 4$). **h** Flow cytometric analysis of neutrophils in steady-state lung, asthmatic lung, and asthmatic BALF after intravenous administration of anti-CD45 antibodies. **i**, Representative histograms showing Siglec-F and PECAM-1 expression in CD45 i.v.$^{-}$ and CD45 i.v.$^{+}$ neutrophils from HDM-induced asthmatic lungs of *Epx*$^{Cre/+}$ and *Epx*$^{Cre/+}$*Gpr43*$^{fl/fl}$ mice. Data in (**f**–**i**) are representative of more than three independent experiments. Data are presented as mean ± s.e.m. Statistical analysis was performed using an unpaired two-tailed Student's t-test (**f, g**). ns, not significant.

Cluster 1, namely, *Siglecf*, *Pecam1*, *Havcr2*, *Scimp*, *Gpr84*, and *Tmem273* (Fig. 3d and Supplementary Fig. 3a). Siglec-F was particularly interesting because, while it often serves as an eosinophil marker, recent studies have identified Siglec-F-expressing neutrophil subsets in diverse diseases, including lung adenocarcinoma, myocardial infarction, and diesel exhaust particle (DEP)-induced lung inflammation[33–35]. Transcriptomic analyses revealed that many genes upregulated in Siglec-F^{hi} neutrophils (relative to Siglec-F^{lo} neutrophils) in these conditions were also highly enriched in our Cluster 1 neutrophils, suggesting potential functional similarities (Supplementary Fig. 3b). In DEP-induced lung inflammation, Siglec-F^{hi} neutrophils actively produced neutrophil extracellular traps (NETs) and promoted the accumulation of type 2 cytokine-producing cells in the lung[35]. Moreover, neutrophils expressing Siglec-8 (the human paralog of murine Siglec-F) are present in the sputum of asthma patients, and their frequency in peripheral blood positively correlates with asthma severity[35]. These observations suggest that the Siglec-F-expressing neutrophils enriched in the asthmatic lungs of *Epx*$^{Cre/+}$*Gpr43*$^{fl/fl}$ mice may also be pathogenic.

Neutrophils in Cluster 0 (Siglec-F^{lo}) were derived from both *Epx*$^{Cre/+}$ and *Epx*$^{Cre/+}$*Gpr43*$^{fl/fl}$ mice at approximately a 1:1 ratio, whereas the majority of Cluster 1 (Siglec-F^{hi}) neutrophils originated from *Epx*$^{Cre/+}$*Gpr43*$^{fl/fl}$ mice (Fig. 3e). This enrichment of Siglec-F-expressing neutrophils in asthmatic lungs of *Epx*$^{Cre/+}$*Gpr43*$^{fl/fl}$ mice was confirmed by flow cytometry (Fig. 3f and Supplementary Fig. 16e). Because *Pecam1* was among the most highly upregulated genes in Cluster 1 neutrophils compared to Cluster 0 neutrophils (Fig. 3d and Supplementary Fig. 3a), we also examined PECAM-1 protein expression. PECAM-1-expressing neutrophils were increased in the asthmatic lungs of *Epx*$^{Cre/+}$*Gpr43*$^{fl/fl}$ mice relative to *Epx*$^{Cre/+}$ mice, and a large proportion of Siglec-F-expressing neutrophils co-expressed PECAM-1 (Fig. 3f). These neutrophils expressing either Siglec-F or PECAM-1 (hereafter referred to simply as Siglec-F^{hi} neutrophils) were almost exclusively found in asthmatic lungs and BALF, whereas few were present in healthy lungs or in the peripheral blood of either healthy or asthmatic mice (Fig. 3g). Additionally, the frequencies of Siglec-F^{hi} neutrophils were significantly higher in the BALF than in the lungs (Fig. 3g). Thus, Siglec-F^{hi} neutrophils likely differentiate from Siglec-F^{lo} neutrophils in the lung during airway inflammation and infiltrate the airway more efficiently. This was supported by in vivo labeling of circulating neutrophils with intravenously injected CD45 antibodies just before sacrifice: none of Siglec-F^{hi} neutrophils in the asthmatic lungs and BALF were labeled with anti-CD45 antibodies (Fig. 3h, i). Thus, during airway inflammation, Siglec-F^{hi} neutrophils are exclusively localized in the lung tissue and exudate, but not in its microvasculature[36].

We also examined the role of GPR43 in eosinophils using an OVA-induced asthma model. Similar to the HDM-induced asthma model, eosinophil-specific deletion of GPR43 exacerbated OVA-induced airway inflammation, which was accompanied by enhanced Th17 responses and increased frequencies of Siglec-F^{hi} neutrophils in the lungs (Supplementary Fig. 4), indicating that this phenomenon is not restricted to a specific model of airway inflammation. Furthermore, global GPR43 knockout mice also exhibited more severe HDM-induced airway inflammation, characterized by simultaneous increases in Th2 and Th17 responses as well as elevated proportion of Siglec-F^{hi} neutrophils in the lungs (Supplementary Fig. 5). Under steady-state conditions, the abundance of Siglec-F^{hi} neutrophils, as well as Th2 and Th17 cells in the lung, was minimal and comparable between *Epx*$^{Cre/+}$ and *Epx*$^{Cre/+}$Gpr43$^{fl/fl}$ mice (Supplementary Fig. 6).

GPR43-deficient eosinophils directly induce the differentiation of Siglec-F^{hi} neutrophils

We next asked how the lack of GPR43 in eosinophils caused the emergence of Siglec-F^{hi} neutrophils during airway inflammation. First, we compared control (EOS^{Ctrl}) and GPR43-deficient eosinophils (EOS$^{\triangle GPR43}$) from the asthmatic lungs of *Epx*$^{Cre/+}$ and *Epx*$^{Cre/+}$*Gpr43*$^{fl/fl}$ mice, respectively. EOS$^{\triangle GPR43}$ were highly vacuolized and exhibited disorganized nuclear shapes (Fig. 4a–c). Eosinophils from patients with severe asthma also have these features[37], which suggests that EOS$^{\triangle GPR43}$ were hyperactivated. The transcriptomic analysis by bulk-RNA sequencing revealed that activated eosinophils expressed multiple chemokines (Supplementary Fig. 7a and Supplementary Data 1). Among them, *Ccl6* and *Cxcl2*, both encoding potent neutrophil chemoattractants[38,39], were the two most highly expressed chemokine genes, suggesting that eosinophils may directly recruit neutrophils in asthmatic lungs. ELISA of culture supernatants from asthmatic lung eosinophils showed that EOS$^{\triangle GPR43}$ produced significantly higher levels of CCL6 and CXCL2 than EOS^{Ctrl}, indicating a greater capacity to attract neutrophils (Fig. 4d, e and Supplementary Fig. 17a). In addition, production of CCL24, a representative eotaxin and another highly expressed chemokine in asthmatic lung eosinophils, was also elevated in EOS$^{\triangle GPR43}$ cells compared with EOS^{Ctrl}, suggesting that the increased eosinophil numbers observed in *Epx*$^{Cre/+}$Gpr43$^{fl/fl}$ mice may be, at least in part, mediated by eosinophil-derived signals (Fig. 4f).

Next, we directly tested whether asthmatic lung eosinophils could attract neutrophils. When EOS^{Ctrl} or EOS$^{\triangle GPR43}$ were cultured with bone marrow-derived neutrophils in a transwell system (Fig. 4g and Supplementary Fig. 17b), neutrophil migration was enhanced by both eosinophils, but especially by EOS$^{\triangle GPR43}$ (Fig. 4h, i). Moreover, unlike neutrophils cultured alone, neutrophils co-cultured with EOS^{Ctrl} or EOS$^{\triangle GPR43}$ formed aggregates, especially with EOS$^{\triangle GPR43}$ (Fig. 4j). Immunofluorescence imaging of the aggregates revealed direct contact between neutrophils and eosinophils, especially with EOS$^{\triangle GPR43}$ (Fig. 4k, l). Immunofluorescence imaging of the asthmatic lung of *Epx*$^{Cre/+}$ mice also showed physical interactions between the neutrophils and eosinophils, especially around the airways (Supplementary Fig. 7b). Thus, eosinophils in the asthmatic lung actively attract and make contact with neutrophils, and this interaction is augmented by GPR43 deficiency in eosinophils. Notably, reanalysis of publicly available transcriptomic data showed that when peripheral blood eosinophils from asthma patients were activated in vitro with IL-33, many neutrophil chemotaxis-related genes were upregulated, implying that human eosinophils can also recruit neutrophils (Supplementary Fig. 7c).

The physical association between eosinophils and neutrophils in asthmatic lungs led us to ask whether eosinophils directly caused Siglec-F^{lo} neutrophils to differentiate into Siglec-F^{hi} neutrophils. Thus,

https://doi.org/10.1038/s41467-025-65573-7

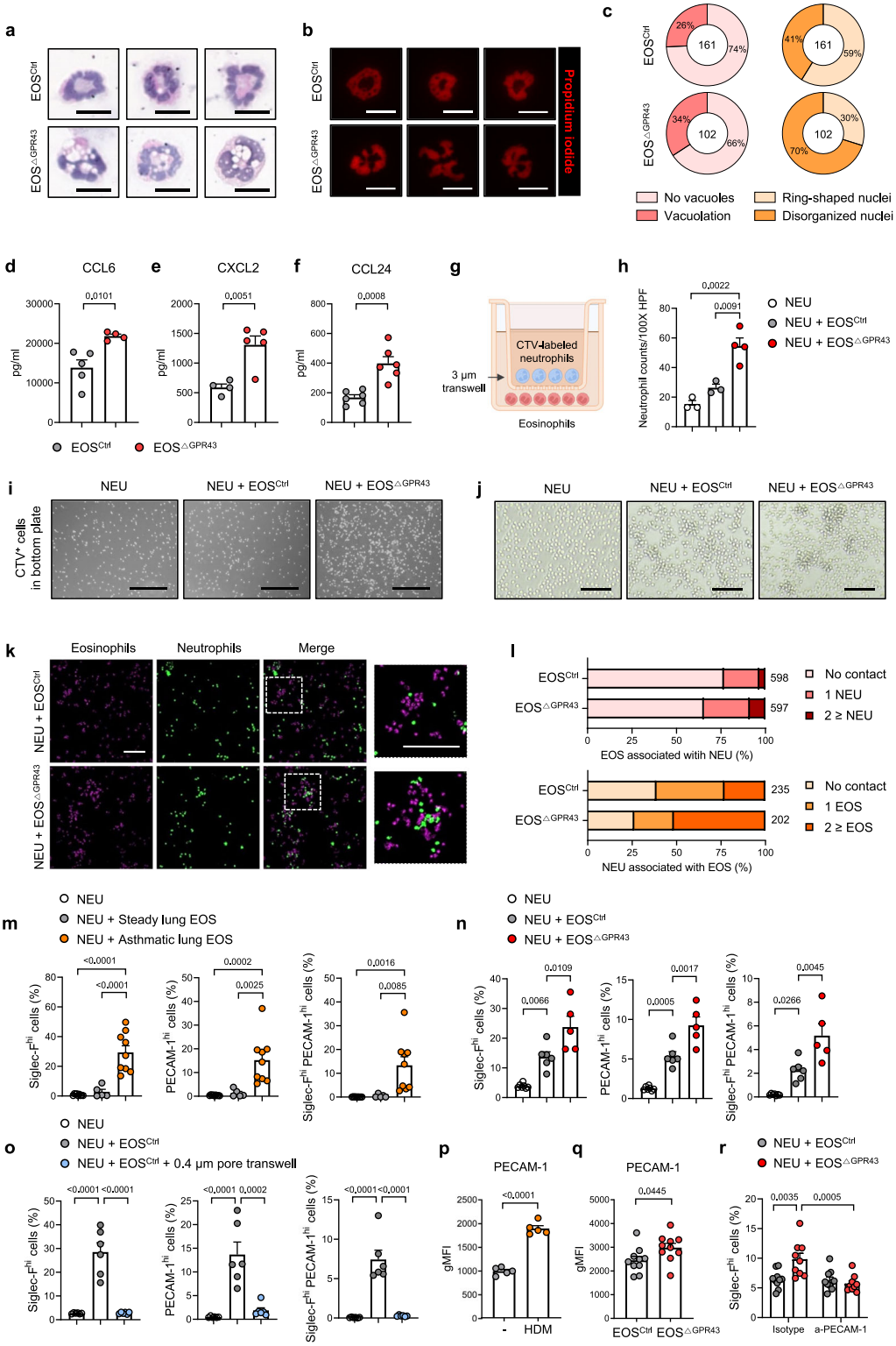

bone marrow neutrophils, which are Siglec-F^{lo}, were co-cultured with eosinophils from asthmatic or healthy lungs of control mice for 2 days. In the absence of eosinophils or in the presence of steady-state lung eosinophils, few Siglec-F^{hi} neutrophils arose (Fig. 4m and Supplementary Fig. 18). In contrast, eosinophils from asthmatic lungs markedly promoted Siglec-F^{hi} neutrophil differentiation, and this effect was further augmented by GPR43 deficiency in eosinophils (Fig. 4m, n). These findings suggest that eosinophils in asthmatic lungs directly drive the emergence of Siglec-F^{hi} neutrophils and that GPR43 deletion in eosinophils exacerbates this process.

Interestingly, eosinophil-mediated differentiation of Siglec-F^{hi} neutrophils was completely abolished when the two cell types were physically separated using a 0.4 µm pore transwell, indicating that direct cell–cell contact is essential (Fig. 4o). Based on this observation, we hypothesized that cell surface adhesion molecules mediating eosinophil–neutrophil interactions may contribute to Siglec-F^{hi} neutrophil differentiation. Notably, we found that asthma induction upregulated PECAM-1 expression in eosinophils, mirroring the upregulation observed in neutrophils (Fig. 4p). Furthermore, eosinophil PECAM-1 expression was higher in EOS$^{\triangle GPR43}$ than in EOS^{Ctrl} (Fig. 4q).

Fig. 4 | GPR43-deficient eosinophils attract neutrophils more efficiently and promote the differentiation of Siglec-F^{hi} neutrophils. a Representative images of H&E-stained asthmatic lung eosinophils from *Epx*$^{Cre/+}$ and *Epx*$^{Cre/+}$*Gpr43*$^{fl/fl}$ mice. Scale bar, 10 μm. **b** Representative images of propidium iodide-stained asthmatic lung eosinophils. Scale bar, 10 μm. **c** Percentages of asthmatic lung eosinophils showing vacuolation (left) and disorganized nuclei (right). Percentages were calculated from three independent H&E images for each group. Total eosinophil numbers are indicated in the centers of the donut plots. **d** CCL6 levels in culture supernatants of asthmatic lung eosinophils. EOS^{Ctrl} ($n = 5$), EOS$^{\triangle GPR43}$ ($n = 4$). **e** CXCL2 levels in culture supernatants of asthmatic lung eosinophils after PMA/Ionomycin stimulation. EOS^{Ctrl} ($n = 4$), EOS$^{\triangle GPR43}$ ($n = 5$). **f** CCL24 levels in culture supernatants of asthmatic lung eosinophils. EOS^{Ctrl} ($n = 6$), EOS$^{\triangle GPR43}$ ($n = 6$). **g** Neutrophil migration assay scheme. Created in BioRender. Yu, J. (2025) https://BioRender.com/lohw7oc. **h** Neutrophil counts within 100x HPF images of the bottom plates. Asthmatic lung eosinophils were pooled from three mice per group for sorting, and assays were performed in technical replicates. NEU ($n = 3$), NEU + EOS^{Ctrl} ($n = 3$), NEU + EOS$^{\triangle GPR43}$ ($n = 4$). **i** Representative images showing CTV-labeled neutrophils migrated toward eosinophils in the bottom plate. Scale bar, 200 μm. **j** Images of eosinophil-neutrophil co-culture. Scale bar, 100 μm. **k** Immunofluorescence images of eosinophil-neutrophil co-culture. Scale bar: 100 μm. **l** Percentages of eosinophils associated with neutrophils (top) and neutrophils associated with eosinophils (bottom). Percentages were calculated from four and three independent fluorescence images for the EOS^{Ctrl} and EOS$^{\triangle GPR43}$ groups, respectively. **m**–**o** Percentages of Siglec-F^{hi}, PECAM-1^{hi}, and Siglec-F^{hi}PECAM-1^{hi} cells among neutrophils. Bone marrow neutrophils were co-cultured with either steady-state eosinophils ($n = 5$) or asthmatic lung eosinophils ($n = 9$) (m); with EOS^{Ctrl} ($n = 6$) or EOS$^{\triangle GPR43}$ ($n = 5$) (n); or with EOS^{Ctrl} in the presence or absence of 0.4 μm transwell ($n = 6$) (o). **p** gMFI of PECAM-1 in eosinophils from steady-state ($n = 5$) and asthmatic lungs ($n = 5$). **q** gMFI of PECAM-1 in asthmatic lung eosinophils. *Epx*$^{Cre/+}$ ($n = 10$), *Epx*$^{Cre/+}$*Gpr43*$^{fl/fl}$ ($n = 10$). **r** Percentages of Siglec-F^{hi}, PECAM-1^{hi}, and Siglec-F^{hi}PECAM-1^{hi} cells among neutrophils after co-culture with eosinophils in the presence or absence of anti-PECAM-1. EOS^{Ctrl} ($n = 10$), EOS$^{\triangle GPR43}$ ($n = 9$). Data in (**m, q, r**) were pooled from two independent experiments. Data are representative of more than two independent experiments. Data are presented as mean ± s.e.m. Statistical analysis was performed using one-way ANOVA (**h, m**–**o**), two-way ANOVA with Tukey's multiple comparison test (r), or unpaired two-tailed Student's t-test (**d**–**f, p, q**). NEU: neutrophils.

PECAM-1 is an adhesion molecule that can mediate the binding of neutrophils to other cells in a homophilic manner[40,41]. To determine whether PECAM-1 participates in eosinophil-induced Siglec-F^{hi} neutrophil differentiation, EOS$^{\triangle GPR43}$ or EOS^{Ctrl} were co-cultured with bone marrow-derived neutrophils in the presence of PECAM-1-blocking antibody. The antibody reduced the ability of EOS$^{\triangle GPR43}$ to induce Siglec-F^{hi} neutrophil differentiation but did not inhibit EOS^{Ctrl}-induced Siglec-F^{hi} neutrophil differentiation (Fig. 4r). This suggests that (i) PECAM-1 proteins overexpressed on EOS$^{\triangle GPR43}$ contribute to the ability of these GPR43-deficient eosinophils to enhance Siglec-F^{hi} neutrophil differentiation, likely by strengthening eosinophil-neutrophil adhesion, but (ii) other mechanisms also mediate these interactions, making PECAM-1 dispensable for Siglec-F^{hi} neutrophil differentiation by EOS^{Ctrl}.

Next, we sought to identify the eosinophil-derived mediators that promote Siglec-F^{hi} neutrophil differentiation. Bone marrow neutrophils were stimulated with various cytokines or LPS. GM-CSF and, to a lesser extent, IL-33, TNF, and LPS, induced Siglec-F expression. By contrast, IL-4 and LPS, and to a lesser extent, IL-33, GM-CSF, and TGFβ, promoted PECAM-1 expression in neutrophils (Fig. 5a). We then combined the cytokines that most strongly stimulated Siglec-F (GM-CSF) and PECAM-1 (IL-4) expression: this combination increased the frequencies of Siglec-F^{hi}, PECAM-1^{hi}, and Siglec-F^{hi}PECAM-1^{hi} neutrophils in a highly synergistic manner (Fig. 5b). This efficient GM-CSF + IL-4-mediated induction of Siglec-F^{hi}, PECAM-1^{hi}, and Siglec-F^{hi}PECAM-1^{hi} neutrophils was also observed when neutrophils from healthy lungs were treated with these cytokines (Fig. 5c). Consistent with these findings, differentiation of neutrophils into Siglec-F^{hi}, PECAM-1^{hi}, and Siglec-F^{hi}PECAM-1^{hi} neutrophils was significantly inhibited by neutralizing antibodies against both IL-4 and GM-CSF, indicating that eosinophil-derived IL-4 and GM-CSF drive Siglec-F^{hi}-neutrophil differentiation (Fig. 5d). IL-4 secretion by asthmatic lung eosinophils was confirmed by ELISA (Supplementary Fig. 7d), whereas GM-CSF was detectable by intracellular cytokine staining but not by ELISA (Supplementary Fig. 7e,19). Unlike neutrophil chemokines, IL-4 and GM-CSF production was comparable between EOS^{Ctrl} and EOS$^{\triangle GPR43}$ (Supplementary Fig. 7d, e), suggesting that the enhanced capacity of GPR43-deficient asthmatic lung eosinophils to promote Siglec-F^{hi}-neutrophil differentiation is mainly attributable to their increased neutrophil recruitment and stronger physical interactions.

Siglec-F^{hi} neutrophils enhance Th17 differentiation

To better characterize Siglec-F^{hi} neutrophils in the HDM-induced asthmatic lung, Cluster 0 (Siglec-F^{lo}) and Cluster 1 (Siglec-F^{hi}) neutrophil transcriptomes were further compared. Relative to Siglec-F^{lo} neutrophils, Siglec-F^{hi} neutrophils demonstrated (i) strong upregulation of cytokine (e.g. *Csf1*, *Tnf*, *Il1a*), chemokine (*Ccl3*, *Ccl4*), degranulation (*Cd63*), and lipid-mediator synthesis (*Ptgs1*, *Ltc4s*) genes, and (ii) downregulation of classical neutrophil function genes (*Lyz2*, *Mmp8*, *S100a8*, *S100a9*, *Ly6g*, *Retnlg*) and a gene related to homing to secondary-lymphoid organs (*Sell*) (Fig. 6a). Gene set enrichment analysis also showed that 'cytokine activity', 'TNF signaling pathway', and 'NF-kappa B signaling pathway' genes were highly enriched in Siglec-F^{hi} neutrophils, as were genes that relate to rheumatoid arthritis and Coronavirus disease-COVID-19 (Fig. 6b and Supplementary Fig. 8). Moreover, Siglec-F^{hi} neutrophils demonstrated enrichment in pattern recognition receptor pathways such as 'NOD-like receptor signaling pathway' and 'C-type lectin receptor signaling pathway' along with'-Phagosome', 'Lysosome', 'Ribosome', 'Oxidative phosphorylation', and 'Apoptosis' genes (Supplementary Fig. 8). Thus, compared to conventional Siglec-F^{lo} neutrophils, Siglec-F^{hi} neutrophils were more activated and likely performed more pro-inflammatory functions.

Closer examination of cytokine expression in Siglec-F^{hi} neutrophils revealed notable increases in *Il1a*, *Il23a*, *Tgfb1*, and *Tnf*, whereas two other Th17-inducing cytokines were either expressed at similar levels in Siglec-F^{hi} and Siglec-F^{lo} neutrophils (*Il1b*) or were poorly expressed in both (*Il6*) (Fig. 6c, d and Supplementary Fig. 9a). Greater expression of TNF and IL-1α in Siglec-F^{hi} neutrophils, along with high but comparable levels of IL-1β in Siglec-F^{hi} and Siglec-F^{lo} neutrophils, was confirmed by ELISA (Supplementary Fig. 9b). Interestingly, of all immune cells in asthmatic lungs, neutrophils were largely the only producers of *Il1a*, *Il23a*, and *Tnf* (Supplementary Fig. 9a). Thus, Siglec-F^{hi} neutrophils may drive Th17 responses. Indeed, Siglec-F^{hi}-neutrophil frequencies in asthmatic lungs correlated positively with RORγt^{+} and IL-17A^{+} CD4 T cell frequencies (Fig. 6e). In contrast, the frequencies of Siglec-F^{lo} neutrophils and dendritic cells showed no correlation with RORγt^{+} and IL-17A^{+} CD4 T cell frequencies (Supplementary Fig. 9c, d).

To determine whether Siglec-F^{hi} neutrophils can directly drive Th17 differentiation, we generated Siglec-F^{hi} neutrophils from Siglec-F^{lo} neutrophils with IL-4 + GM-CSF (Fig. 6f). Like Siglec-F^{hi} neutrophils in asthmatic lungs, these in vitro-generated Siglec-F^{hi} neutrophils expressed high levels of *Il1a, Il23a*, and *Tnf* compared to Siglec-F^{lo} neutrophils (Supplementary Fig. 9e). They also expressed more IL-1α and TNF, as determined by ELISA (Supplementary Fig. 9f). Thus, Siglec-F^{hi} neutrophils generated in vitro with cytokines closely resembled Siglec-F^{hi} neutrophils in asthmatic lungs. Importantly, co-culture with naïve CD4 T cells showed that Siglec-F^{hi} neutrophils significantly enhanced Th17 cell differentiation compared to Siglec-F^{lo} neutrophils, as indicated by higher RORγt^{+} and IL-17A^{+} cell frequencies (Fig. 6f, g).

https://doi.org/10.1038/s41467-025-65573-7

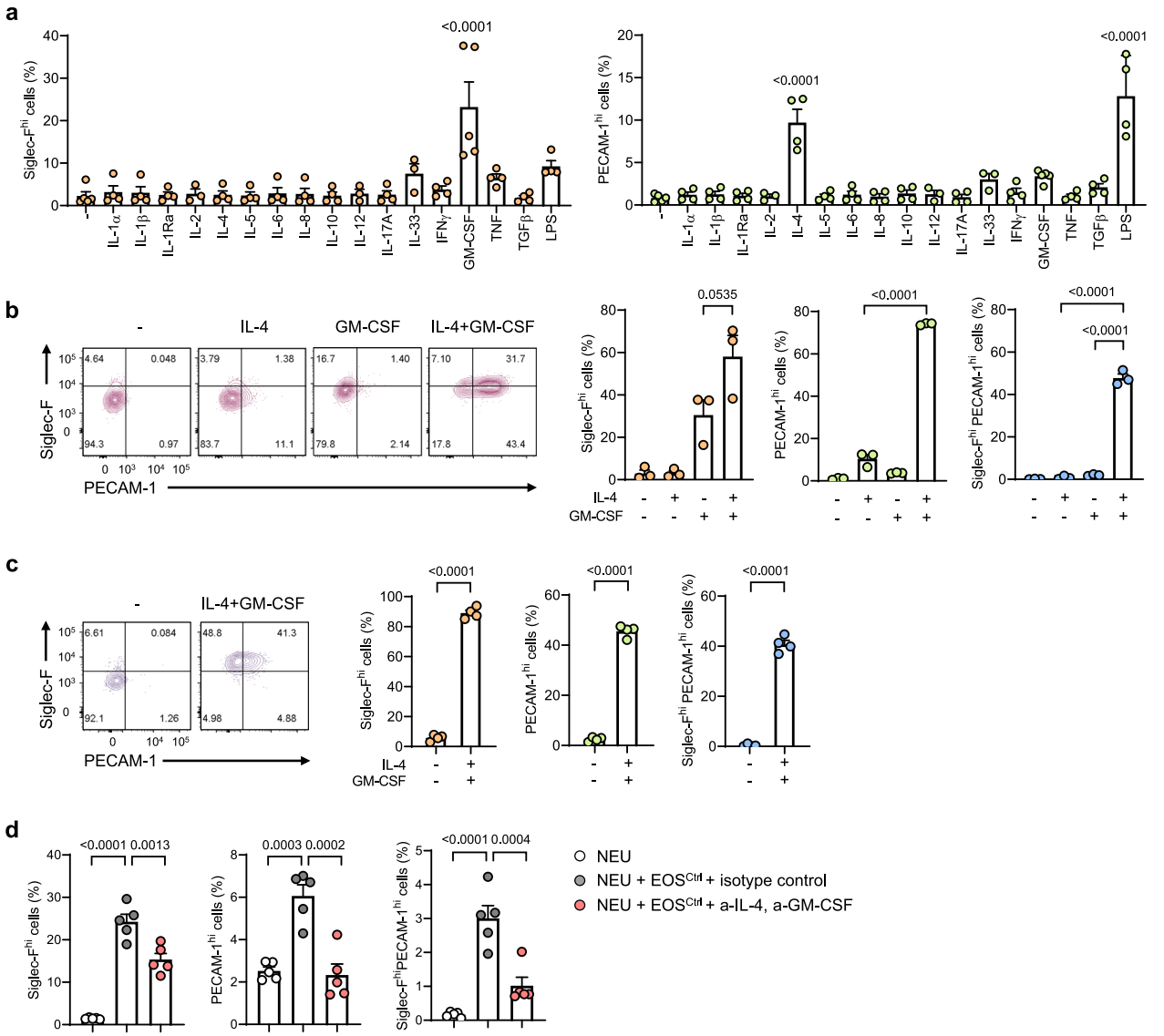

Fig. 5 | Eosinophil-induced differentiation of Siglec-F^{hi} neutrophils is dependent on IL-4 and GM-CSF. Shown are the percentages of Siglec-F^{hi}, PECAM-1^{hi}, and Siglec-F^{hi}PECAM-1^{hi} neutrophils. **a** Bone marrow neutrophils stimulated with various cytokines or LPS ($n = 5$ for untreated and GM-CSF; $n = 3$ for IL-2, IL-12, and IL-33; $n = 4$ for all other groups). Data were pooled from five independent experiments. **b** Bone marrow neutrophils stimulated with IL-4, GM-CSF, or both cytokines ($n = 3$). Data were pooled from three independent experiments. **c** Steady-state lung neutrophils were stimulated with the combination of IL-4 and GM-CSF ($n = 4$). Data are representative of two independent experiments. **d** Bone marrow neutrophils were co-cultured with asthmatic lung eosinophils in the presence of anti-IL-4 plus anti-GM-CSF antibodies or isotype controls ($n = 5$). Data are representative of three independent experiments. Data are presented as mean ± s.e.m. Statistical analysis was performed using one-way ANOVA with Tukey's multiple comparison test (**a, b, d**) and unpaired two-tailed Student's t-test (**c**).

Eosinophils have been shown to modulate CD4 T cell differentiation directly or indirectly by regulating DC functions[7,8,42,43]. Because the frequencies of RORγt$^+$ and IL-17A$^+$ CD4 T cells in asthmatic lungs also positively correlated with eosinophil frequencies (Supplementary Fig. 9c, d), we next asked whether eosinophils, like Siglec-F^{hi} neutrophils, can directly augment Th17 differentiation. However, co-culturing naïve CD4 T cells with EOS^{Ctrl} or EOS$^{\triangle GPR43}$, with or without DCs, showed that while DCs increased Th17 differentiation, eosinophils could neither directly nor indirectly enhance it (Supplementary Fig. 10a, b). This is consistent with the comparable expression in EOS^{Ctrl} and EOS$^{\triangle GPR43}$ of antigen presentation- and Th17 differentiation-related genes (Supplementary Fig. 10c, d), as well as their similar levels of IL-1-receptor antagonist (IL-1Ra), which can suppress Th17 cell differentiation[8] (Supplementary Fig. 10e). Moreover, DCs in asthmatic lungs from *Epx*$^{Cre/+}$ and *Epx*$^{Cre/+}$*Gpr43*$^{fl/fl}$ mice exhibited similar expression of antigen presentation-, Th17 activation-, and Th17 differentiation-related genes (Supplementary Fig. 10f). Collectively, these results suggest that lack of GPR43 in eosinophils induces their hyperreactivity in the asthmatic lung, leading to the generation of Siglec-F^{hi} neutrophils, which then can promote Th17 cell responses.

GPR43 in eosinophils is required for acetate-mediated suppression of Siglec-F^{hi} neutrophils in female mice

Given the well-documented influence of sex on asthma pathogenesis and severity[44–46], we investigated whether female *Epx*$^{Cre/+}$*Gpr43*$^{fl/fl}$ mice also display exacerbated airway inflammation and increased frequencies of Siglec-F^{hi} neutrophils compared with female *Epx*$^{Cre/+}$ controls. When asthma was induced by HDM in male and female mice in parallel, females exhibited greater immune cell infiltration in the BALF and higher lung Siglec-F^{hi} neutrophil frequencies, indicating stronger

https://doi.org/10.1038/s41467-025-65573-7

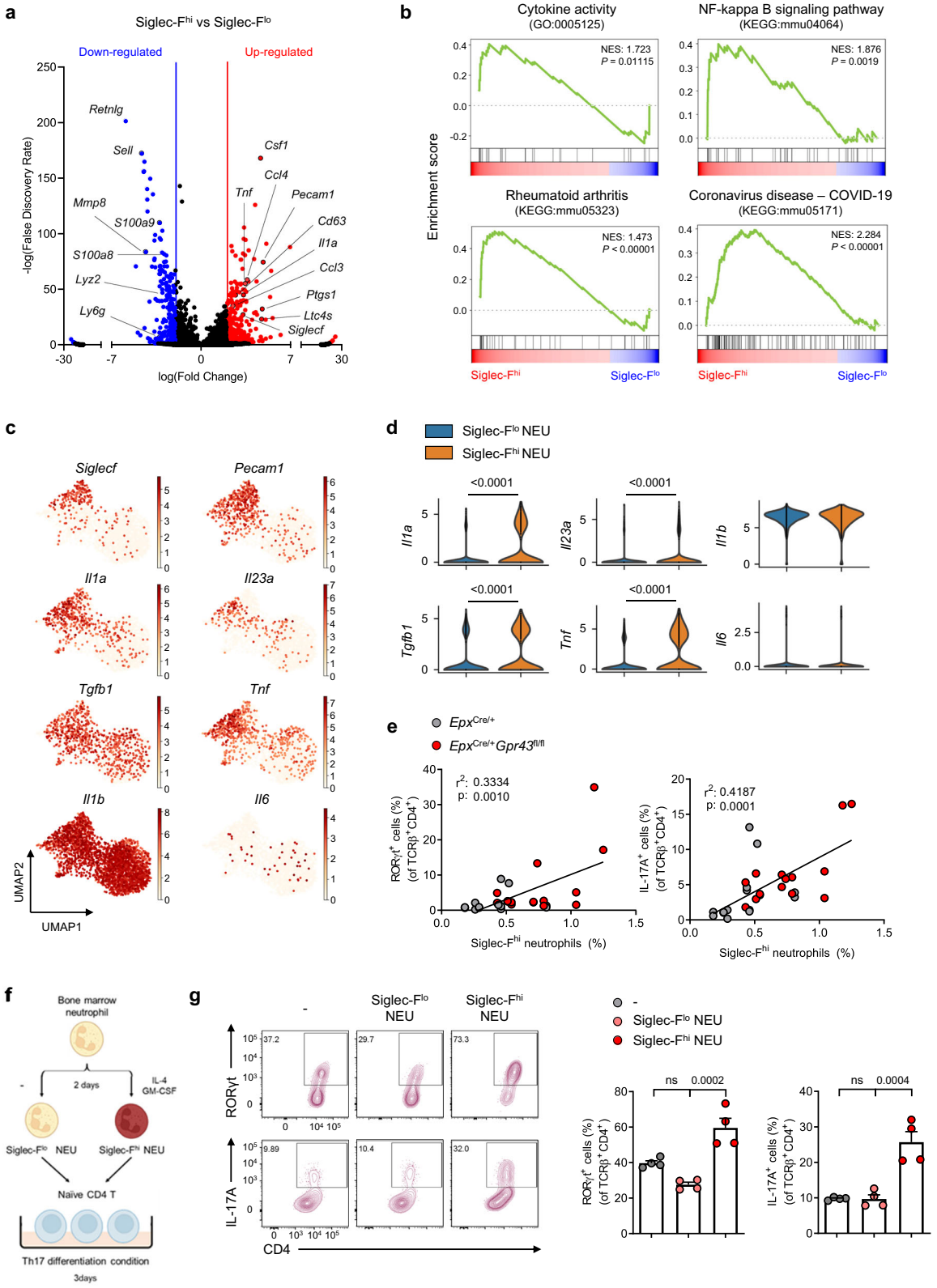

overall immune responses than males (Supplementary Fig. 11a, b). Moreover, unlike males, female *Epx*$^{Cre/+}$ and *Epx*$^{Cre/+}$*Gpr43*$^{fl/fl}$ mice showed no differences in BALF immune cell counts or lung Siglec-F^{hi} neutrophil frequencies. Th2 and Th17 responses were also comparable between the two female genotypes (Supplementary Fig. 11c, d). Similarly, systemic GPR43 deficiency did not alter BALF immune cell counts, lung Siglec-F^{hi} neutrophil frequencies, and Th2 and Th17 responses in female mice (Supplementary Fig. 12).

Nonetheless, administration of acetate, an endogenous GPR43 agonist, during asthma induction in female mice reduced lung Siglec-F^{hi} neutrophil proportions in a GPR43-dependent manner, indicating that GPR43 in eosinophils can suppress Siglec-F^{hi} neutrophil differentiation in females under specific conditions such as elevated SCFA levels (Supplementary Fig. 13). To determine more directly whether GPR43 intrinsically regulates female eosinophil function without potential confounding effects of the in vivo environment, we analyzed

Fig. 6 | Siglec-F^{hi} neutrophils enhance the differentiation of Th17 cells. a Volcano plot displaying differential gene expression between Siglec-F^{lo} and Siglec-F^{hi} neutrophils (FDR < 0.05, absolute logFC > 2 highlighted). **b** Gene set enrichment analysis of differentially expressed genes. **c, d** UMAP plots (**c**) and violin plots (**d**) for cytokine genes related to Th17 differentiation. **e** Correlation between the proportion of Siglec-F^{hi} neutrophils and RORγt^{+} or IL-17A^{+} CD4 T cells in asthmatic lungs. *Epx*$^{Cre/+}$ ($n = 14$), *Epx*$^{Cre/+}$*Gpr43*$^{fl/fl}$ ($n = 15$). Data were pooled from three independent experiments. **f** Experimental scheme for co-culture of neutrophils and naïve CD4 T cells under Th17 differentiation conditions. Created in BioRender. Yu, J. (2025) https://BioRender.com/j8a0ji3. Siglec-F^{lo} and Siglec-F^{hi} neutrophils were prepared by culturing bone marrow neutrophils in the absence or presence of IL-4 and GM-CSF, respectively. **g** Percentages of RORγt^{+} and IL-17A^{+} CD4 T cells after the co-culture. Siglec-F^{lo} neutrophils ($n = 4$), Siglec-F^{hi} neutrophils ($n = 4$). Data are representative of three independent experiments. Data are presented as mean ± s.e.m. Statistical analysis was performed using a two-sided permutation test with false discovery rate (FDR) correction for multiple comparison (**b**), the Wilcoxon rank-sum test with Benjamini–Hochberg correction (**d**), simple linear regression (**e**), and one-way ANOVA with Tukey's multiple comparison test (**g**). ns, not significant.

chemokine production by bone marrow–derived eosinophils (BMDEs) from *Epx*$^{Cre/+}$ and *Epx*$^{Cre/+}$*Gpr43*$^{fl/fl}$ mice. Consistent with findings in male asthmatic lung eosinophils, GPR43 deficiency increased chemokine production in male BMDEs stimulated with IL-33 (Supplementary Fig. 14). Likewise, GPR43-deficient female BMDEs secreted higher levels of CCL6 and CCL24, although CXCL2 production was unaffected (Supplementary Fig. 14). Collectively, these results demonstrate that GPR43 intrinsically modulates eosinophil function in both sexes, but functional differences between control and GPR43-deficient female eosinophils can be masked in vivo by cell-extrinsic factors, especially under highly inflammatory conditions.

Discussion

GPR43 plays anti-inflammatory roles in various inflammatory diseases, and multiple cell types can mediate this activity. Here, we demonstrate that GPR43 also plays anti-inflammatory roles in eosinophils. Upon induction of allergic airway inflammation, eosinophils lacking GPR43 became hyperactive, leading to enhanced type 2 immune responses. This was reflected by increased frequencies of both eosinophils and Th2 cells, which together contributed to elevated type 2 cytokine levels. Our in vitro and in vivo observations further suggest that eosinophil hyperactivity also drove excessive differentiation of Siglec-F^{hi} neutrophils, which in turn increased Th17 cells in the lung and exacerbated airway inflammation.

Eosinophils interact with and control diverse immune cell types. However, whether eosinophils can regulate neutrophils, particularly directly, has been poorly studied[47,48], likely because eosinophils and neutrophils play canonical roles in type 2 and type 3 immunity, respectively[49]. Our study showed that eosinophils can, in fact, directly regulate neutrophils in several ways. First, even normal lung eosinophils (with GPR43) from asthmatic mice could recruit neutrophils by producing neutrophil chemoattractants. Moreover, our re-analysis of publicly available bulk RNA-seq data showed that when human eosinophils are treated with the asthma-promoting cytokine IL-33, they express multiple neutrophil chemoattractants. This potential for direct neutrophil attraction by eosinophils has also been observed in other inflammatory settings[50]. Second, we observed that eosinophils interacted physically with neutrophils, both in vitro and in vivo, and that this led to their differentiation into Siglec-F^{hi} neutrophils. Both mechanisms were elevated when eosinophils lacked GPR43, which suggests that GPR43 constitutively prevents eosinophils from recruiting neutrophils and converting them into more pathogenic Siglec-F^{hi} neutrophils.

The eosinophil-induced differentiation of Siglec-F^{hi} neutrophils was likely mediated by eosinophil-derived IL-4 and GM-CSF, since differentiation was largely blocked by antibodies against these cytokines. Surprisingly, despite the involvement of these soluble factors, direct physical interaction between the two cell types was indispensable for Siglec-F^{hi} neutrophil differentiation. Given that asthmatic lung eosinophils produced relatively low levels of IL-4 and GM-CSF, direct contact may represent the most efficient means of delivering these limited cytokines. Moreover, the comparable IL-4 and GM-CSF levels in control and GPR43-deficient eosinophils suggest that stronger chemoattraction and an increased likelihood of physical contact are the key factors driving the enhanced differentiation observed in the absence of GPR43 in eosinophils.

In vivo, additional mechanisms are likely to contribute. For example, the increased eosinophil numbers in *Epx*$^{Cre/+}$*Gpr43*$^{fl/fl}$ mice could elevate total IL-4 and GM-CSF levels within the asthmatic lung environment. Other cellular sources, including Th2 cells and ILC2s, may also supply these cytokines; notably, IL-4–producing CD4 T cells were increased in *Epx*$^{Cre/+}$*Gpr43*$^{fl/fl}$ mice. Furthermore, other soluble factors may also contribute. Previous studies have shown that ATP and TGFβ can also promote Siglec-F^{hi} neutrophil differentiation[35,51]. We also found that IL-33 and TNF can generate Siglec-F^{hi} neutrophils, albeit less well than GM-CSF. Further identification of the signals required for in vivo generation of Siglec-F^{hi} neutrophils in allergic airway inflammation will be important.

We found that many Siglec-F^{hi} neutrophils in the asthmatic lungs and BALF co-expressed PECAM-1. Siglec-F^{hi}PECAM-1^{hi} neutrophils were also generated in vitro from Siglec-F^{lo}PECAM-1^{lo} neutrophils by asthmatic lung eosinophils, especially GPR43-deficient eosinophils. Notably, PECAM-1 co-expression by Siglec-F^{hi} neutrophils has not been observed elsewhere, including in lung adenocarcinoma[33], myocardial infarction[34], and DEP-induced lung inflammation[35]. Since IL-4 was by far the most potent PECAM-1-upregulating cytokine among the 16 cytokines tested, PECAM-1 co-expression by Siglec-F^{hi} neutrophils may be unique to type 2 cytokine-rich inflammatory conditions. However, we found that LPS, GM-CSF, and IL-33 also induced PECAM-1 expression. Thus, PECAM-1 could potentially be upregulated in Siglec-F^{hi} neutrophils in other inflammatory conditions.

Since asthmatic lung eosinophils also express PECAM-1, and this is upregulated by GPR43 deletion, we speculated that homophilic PECAM-1 interactions induce binding of neutrophils to eosinophils and contribute to Siglec-F^{hi} neutrophil induction. However, PECAM-1-blocking antibody only suppressed the enhanced ability of EOS$^{\triangle GPR43}$ to induce Siglec-F^{hi} neutrophil differentiation: it did not suppress baseline EOS^{Ctrl}-induced Siglec-F^{hi} neutrophil differentiation. Therefore, other adhesion molecules appear to play a greater role in the physical interaction between eosinophils and neutrophils, especially in the early phase of their interactions, while overexpressed PECAM-1 in EOS$^{\triangle GPR43}$ further enhances the interactions. Another possibility is that PECAM-1-mediated signaling events participate in the eosinophil-induced neutrophil differentiation: the cytoplasmic tail of PECAM-1 bears immunoreceptor tyrosine-inhibitory motifs, and PECAM-1 can modulate immune cell intracellular signaling[41,52]. Further studies are needed to identify additional molecules mediating the direct eosinophil-neutrophil interaction and to determine the exact mechanism(s) by which PECAM-1 regulates eosinophil-induced Siglec-F^{hi}-neutrophil differentiation.

Notably, asthmatic lungs also bore neutrophils that expressed PECAM-1 but not Siglec-F (Fig. 3f). Moreover, none of the PECAM-1^{hi} or Siglec-F^{hi} neutrophils were found in the circulation (Fig. 3g–i). In addition, genes related to Th17 differentiation[53,54] were upregulated in Siglec-F^{hi} neutrophils, and they could enhance Th17 cell differentiation. These findings, together with the production of neutrophil chemoattractants by eosinophils in asthmatic lungs, suggest the following sequence of immunological events in asthmatic lungs: (1) PECAM-1^{lo}

https://doi.org/10.1038/s41467-025-65573-7

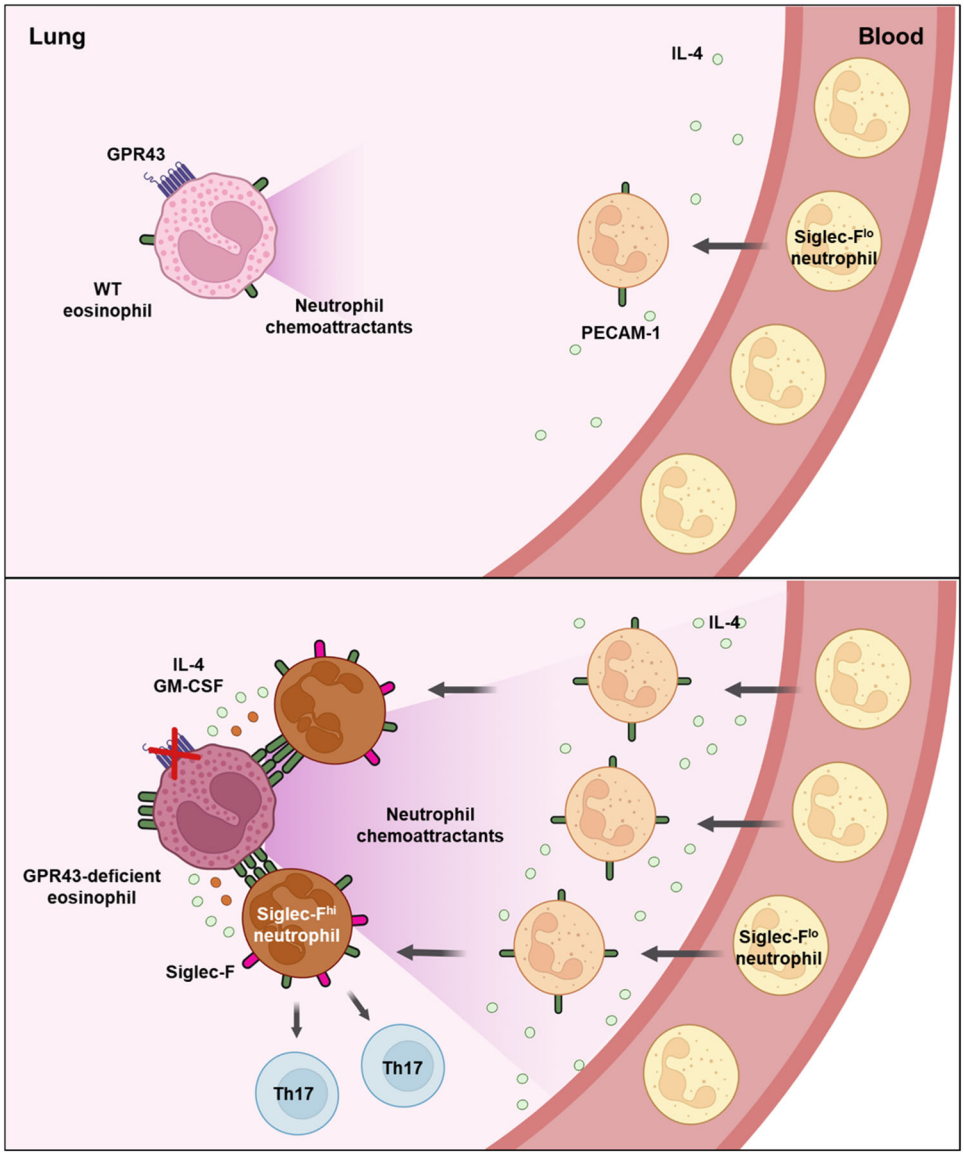

Fig. 7 | Schematic of eosinophil-mediated Siglec-F^{hi} neutrophil induction in asthmatic lungs. (Top) In wild-type mice, GPR43 restrains eosinophil activation and the production of neutrophil chemoattractants, resulting in limited neutrophil recruitment and minimizing the generation of Siglec-F^{hi} neutrophils. (Bottom) In eosinophil-specific GPR43-deficient mice, infiltrating neutrophils are exposed to elevated levels of IL-4 and upregulate PECAM-1 expression. GPR43-deficient eosinophils are hyperactivated, produce more neutrophil chemoattractants, and express higher levels of PECAM-1 compared with wild-type eosinophils. These changes lead to enhanced neutrophil recruitment and stronger eosinophil-neutrophil interactions, promoting the induction of Siglec-F^{hi} neutrophils via eosinophil-derived IL-4 and GM-CSF. Siglec-F^{hi} neutrophils, in turn, promote Th17 cell differentiation. Created in BioRender. Yu, J. (2025) https://BioRender.com/d0uv25k.

neutrophils enter the lung from blood, partly due to eosinophil-derived chemokines such as CCL6 and CXCL2, (2) the IL-4-rich local environment induces neutrophil expression of PECAM-1, (3) the eosinophil-derived chemokines further encourage the neutrophils to approach and physically connect with the eosinophils and the local eosinophil-derived IL-4 further increases PECAM-1 expression on the neutrophils, (4) eosinophil-derived IL-4 + GM-CSF induces Siglec-F expression (i.e. differentiation) of the neutrophils, and (5) Siglec-F^{hi} neutrophils promote Th17 differentiation (Fig. 7). This whole process can potentially occur in the asthmatic *Epx*$^{Cre/+}$ lung but significantly worsens when GPR43 is deleted in eosinophils because the deletion increases eosinophil-mediated neutrophil chemoattraction and eosinophil PECAM-1 expression. Consequently, EOS$^{\triangle GPR43}$ attracts more neutrophils and converts them to Siglec-F^{hi} neutrophils. Therefore, eosinophil-expressed GPR43 downregulates crosstalk between eosinophils and neutrophils in asthma-induced lung inflammation, thus minimizing eosinophil-mediated induction of Siglec-F^{hi} neutrophils.

Siglec-F^{hi} neutrophils have been found to play pathogenic roles in many diseases[33–36]. Similarly, Siglec-F^{hi} neutrophils in our HDM-induced asthma model highly expressed proinflammatory genes, especially *Il1a* and *Il23a*, promoting Th17 cells[53,54]. Since Th17 cells and IL-17A can, in turn, promote neutrophil-mediated immune responses[55,56], it is possible that there is a positive feedback loop between Siglec-F^{hi} neutrophils and Th17 cells that results in exacerbated asthma symptoms. Moreover, this feedback loop can be strengthened when GPR43 is deleted in eosinophils.

While most of these mechanisms were studied in male mice, enhanced production of chemokines, particularly CCL6 and CCL24, was also observed in GPR43-deficient female eosinophils. Moreover,

under acetate-treated asthma conditions, female *Epx*$^{Cre/+}$*Gpr43*$^{fl/fl}$ mice exhibited higher frequencies of Siglec-F^{hi} neutrophils than control females, indicating that the role of eosinophil GPR43 is conserved across sexes. Nonetheless, several other phenotypic differences observed between male *Epx*$^{Cre/+}$ and *Epx*$^{Cre/+}$*Gpr43*$^{fl/fl}$ mice were not evident in females, revealing notable sex-specific variations. Sex-based differences in asthma pathogenesis, including more severe inflammation, have been widely reported[44–46]. Proposed contributing factors include hormonal influences[57–59], structural differences in lung anatomy[60], and gut microbiota composition[61–63]. In addition, systemic SCFA levels differ between males and females under both steady-state and disease conditions[64–66], although whether such differences occur during asthma remains unknown. These variables may influence the magnitude or context-dependence of GPR43 signaling. Further investigation is needed to elucidate how sex-specific physiological factors intersect with GPR43-mediated regulation of eosinophil–neutrophil interactions in allergic airway inflammation.

Beyond these mechanistic and sex-specific insights, our findings are of clinical interest because asthma is broadly classified on the basis of immune cell profiles as eosinophilic and non-eosinophilic asthma[67,68]. Eosinophilic asthma is driven by Th2 responses and is generally readily managed with corticosteroids. Non-eosinophilic asthma includes the neutrophilic and paucigranulocytic endotypes and associates with either Th1 or Th17 responses. It is often resistant to corticosteroid treatment. Non-eosinophilic asthma also includes the mixed-granulocytic endotype, which involves both eosinophils and neutrophils and is driven by Th2 and Th17 response: this endotype is associated with severe symptoms[69–71]. Since we found that eosinophils directly regulate neutrophils and GPR43 is a critical suppressor of eosinophil hyperactivation, our results offer valuable insights into mechanisms that may underlie the development of mixed-granulocytic asthma. For example, our findings suggest that insufficient GPR43 signaling due to antibiotic overuse or inadequate dietary fiber intake could induce dysfunctional eosinophils that aberrantly recruit and activate neutrophils in response to asthmogenic signals, which in turn trigger powerful Th17 responses. Further studies on the GPR43-eosinophil-Siglec-F^{hi} neutrophil-Th17 axis in not only asthma but also other diseases that involve both eosinophils and neutrophils (e.g., chronic obstructive pulmonary disease, infections, and tumors) are warranted.

Methods

Experimental animals

Gpr43$^{fl/fl}$ mice were generated using ES cells (Ffar2tm1a(EUCOMM) Hmgu, Clone # HEPD0778_6_G06) from EUCOMM. *Epx*-Cre mice[72] and Rosa26-eYFP$^{fl/fl}$ mice (Jackson laboratory, 006148)[73] were obtained from the late James J. Lee (Mayo Clinic, Rochester, Minnesota, USA) and Suk-jo Kang (Korea Advanced Institute of Science and Technology (KAIST), Daejeon, Republic of Korea), respectively. GPR43$^{-/-}$ mice were previously described[74]. All mice were maintained on a C57BL/6 background. Control and experimental groups were co-housed from three weeks of age until the end of the experiments. Unless otherwise stated, all experiments were performed using eight to thirteen-week-old male mice. Mice were provided with standard chow *ad libitum* and maintained under specific pathogen-free conditions at 22 ± 2 °C, 50 ± 10% humidity, with a 12-h light-dark cycle in the KAIST Laboratory Animal Resource Center. All mouse experiments were approved by the KAIST Institutional Animal Care and Use Committee (IACUC).

Allergic airway inflammation models

For the HDM-induced asthma model, mice received intranasal administration of 10 μl of 1 mg/ml house dust mite (HDM) extract (Greer, USA, Catalogue#XPB82D3A2.5) dissolved in PBS on days 0, 7, 8, 9, 10, and 11. For acetate treatment, sodium acetate (Sigma-Aldrich, USA, Catalogue#S5636) was dissolved in water, adjusted to pH 7.4, and administered intraperitoneally at 0.5 g/kg body weight 30 minutes before HDM administration on days 7-11. For the OVA-induced asthma model, mice were sensitized intraperitoneally on day 0 with 200 μl of 1 mg/ml OVA (Sigma-Aldrich, USA, Catalogue#A5503) and Alum (Imject, USA, Catalogue#77161) mixed in a 1:1 ratio. Mice were then challenged intranasally with 20 μl of 2.5 mg/ml OVA in PBS on days 7, 8, and 9. For all intranasal administration, mice were anesthetized by intraperitoneal injection of a mixture containing ketamine (80 mg/kg) and rompun (4 mg/kg) in PBS. In both models, mice were euthanized using CO_2 one day after the last challenge.

Measurement of airway resistance

Airway resistance was measured using FlexiVent (SCIREQ, Canada). Mice were anesthetized by intraperitoneal injection of pentobarbital sodium solution in PBS (30 mg/kg) and intubated with 20-gauge catheters by tracheostomy. To block spontaneous breathing, 100 μl of 1 μg/ml pancuronium bromide (Sigma-Aldrich, Catalogue#P1918) was injected intraperitoneally. Mice were mechanically ventilated at a tidal volume of 10 ml/kg and a respiratory rate of 150/min. Respiratory resistance (Rrs) values were acquired after administering increasing doses (0, 5, 10, 20 mg/ml) of aerosolized methacholine (Sigma-Aldrich, Catalogue# A2251).

Histological analysis of asthmatic lung

Half of the left lung tissues were excised, fixed with 3.7% formaldehyde (Sigma-Aldrich, Catalogue#F1635) at 4 °C overnight, and embedded in paraffin using a tissue processor (TP1020 Automatic Benchtop Tissue Processor / HistoCore Arcadia, Leica). The paraffin block was cut into 10 μm-thick sections with the microtome (RM2235, Leica) and stained with hematoxylin (Merck, Germany, Catalogue#1.09253.1000) and eosin (Merck, Catalogue#1.09844.1000) using a standardized protocol. Periodic Acid Schiff (PAS) and Picro Sirius Red staining were performed using kits (Abcam, UK, Catalogue#ABC-AB150680, ABC-AB150681) according to the manufacturer's protocols. Images were obtained using a slide scanner (Pannoramic SCAN II, 3DHISTECH, Hungary) in the EM & histology core facility at the KAIST biomedical research center.

Immunofluorescence imaging of asthmatic lung

After euthanizing the mice, 1 ml OCT solution (Sakura Finetek, USA, Catalogue#4583) was injected into the lungs through the trachea, and the lungs were extracted. The extracted lungs were immersed in OCT solution and preserved at -20 °C. OCT-embedded lungs were sectioned into 14 μm-thick slices and attached to the slide glasses. After fixation with 4% paraformaldehyde (Sigma-Aldrich, Catalogue#P6148) and permeabilization with 0.3% Triton X-100 in PBS, anti-Siglec-F (E50-2440, BD Biosciences, Catalogue#55125) and anti-myeloperoxidase (P11247, R&D Systems, Catalogue#AF3667) antibodies were used to stain eosinophils and neutrophils, respectively. Anti-rat IgG-AF594 (Thermo Fisher Scientific, Catalogue#A-21209) and anti-goat IgG-AF488 (Thermo Fisher Scientific, Catalogue#A-11055) antibodies were used as the secondary antibodies. After nuclear staining with DAPI (Thermo Fisher Scientific, Catalogue#D1306) and adding a fluorescence mounting medium (Dako, Denmark, Catalogue#S3020), a cover glass was mounted. Confocal imaging was performed using Nikon A1 HD25 microscope (Japan), and images were processed with NIS-Elements BR 4.60. software.

Lung and BALF cell preparation

Lungs were chopped into 1 mm^3 fragments and digested with 400 MandlU/ml collagenase D (Roche, Switzerland, Catalogue#11088882001) and 10 μg/ml DNase I (Roche, Catalogue#10104159001) in RPMI1640 media (Welgene, South Korea, Catalogue#LM011-01) containing 3% FBS (Atlas biologicals, USA,

Catalogue#EF-0500-A), 20 mM HEPES (Welgene, Catalogue#BB001-01), 1 mM non-essential amino acids (Welgene, Catalogue #LS005-01), 100 U/ml penicillin, 100 μg/ml streptomycin (Welgene, Catalogue#LS 202-02), and 1 mM sodium pyruvate (Welgene, Catalogue#LS013-01) at 37 °C for 30 min with stirring. The enzyme reaction was stopped by adding 10 μl of 0.5 M EDTA (Sigma-Aldrich, Catalogue#E6758) and incubating the cells for an additional 5 min. After vigorous resuspension, the cells were filtered through 100 μm strainers (SPL, South Korea, Catalogue#93100). Red blood cells were lysed with ACK lysis buffer containing 0.15 M NH_4Cl (Daejung, South Korea, Catalogue#1060-4405), 10 mM $KHCO_3$ (Daejung, Catalogue#6580-4405), and 0.1 mM EDTA (Sigma-Aldrich, Catalogue#E6758) for 3 min at room temperature. BALF was collected by flushing the airways with 1 ml PBS. To evaluate the tissue localization of immune cells by flow cytometry, mice were injected intravenously with 1 μg of CD45-PE antibody (30-F11, Biolegend, Catalogue#103106) 5 min before sacrifice.

Flow cytometry

Cells were first stained with Ghost dye violet 510 (Tonbo, USA, Catalogue#13-0870-T500) for live/dead staining and then with fluorescent dye-labeled antibodies in PBS-based buffer supplemented with 3 % FBS, 1 mM EDTA, and 20 mM HEPES on ice for 20 min. For intracellular cytokine staining, the cells were stimulated with a cocktail containing 81 nM PMA (Sigma-Aldrich, Catalogue#79346), 1.34 μM ionomycin (Sigma-Aldrich, Catalogue#I9657), 2 μM monensin (Sigma-Aldrich, Catalogue#M5273), and 10.6 μM brefeldin A (Sigma-Aldrich, Catalogue#B7651) at 37 °C for 4 h. The cells were then fixed and permeabilized with 3.7% formaldehyde (Sigma-Aldrich, Catalogue#F1635) and 0.5% saponin (Sigma-Aldrich, Catalogue#47036), respectively. To stain the transcription factors in CD4 T cells, a FoxP3 staining kit (eBioscience, Catalogue#00-5521-00) was used according to the manufacturer's protocol. All antibodies used for flow cytometry analysis are detailed in Supplementary Table 1. Flow cytometric analysis was performed using BD Biosciences LSR Fortessa X-20 and data were analyzed with BD Biosciences Flowjo v.10.10.0. Gating strategies can be found in Supplementary Figs. 15–19.

Purification of lung eosinophils and morphological analysis

After staining lung cells with fluorescent dye-labeled antibodies, eosinophils were purified by fluorescence-activated cell sorting using BD Biosciences Aria Fusion. Dead cells were excluded using propidium iodide staining. The purity of the sorted eosinophils was over 95% (Supplementary Fig. 17a). For morphological analysis, 50,000 cells were attached to a slide glass using Cytospin 4 (Thermo Fisher Scientific). After overnight drying, cells were fixed with 3.7% formaldehyde, stained with hematoxylin and eosin using a standardized protocol, and mounted with xylene mounting solution (BBC Biochemical, USA). To analyze their nuclear shape, cells were stained with propidium iodide and mounted with a fluorescence mounting medium (Dako). The images were taken with Pannoramic SCAN II.

Purification of bone marrow and lung neutrophils

To purify bone marrow neutrophils, bone marrow cells were collected by flushing the tibia and femur with RPMI1640-based media containing 2% FBS (Atlas Biologicals), 10 mM HEPES, 100 U/ml penicillin, and 100 μg/ml streptomycin using 26 G syringes. The bone marrow and lung cell preparations were enriched for neutrophils by negative selection with biotin-conjugated antibodies listed in Supplementary Table 2 by using EasySep Mouse Streptavidin RapidSpheres isolation kit (STEMCELL Technologies, Catalogue#ST19860). The neutrophils were further stained with fluorescent dye-labeled antibodies and purified using an Aria Fusion cell sorter (BD Biosciences). Their purity was over 95% (Supplementary Fig. 17b).

In vitro differentiation of Siglec-F^{hi} neutrophils

For cytokine-induced differentiation of Siglec-F^{hi} neutrophils, 0.2 million neutrophils purified from the bone marrow were cultured in RPMI-based media supplemented with 10% FBS (Hyclone, Catalogue#SH30919.03), 1 mM non-essential amino acids, 5 mM HEPES, 100 U/ml Penicillin, 100 μg/ml Streptomycin, 1 mM sodium pyruvate, 50 μg/ml gentamicin (Gibco, USA, Catalogue#15750-060), 55 μM β-mercaptoethanol (Sigma-Aldrich, Catalogue#M6250), and 2 mM L-glutamine (Gibco, Catalogue#25030-081) for 2 days in the presence of 10 ng/ml of each cytokine, including IL-1α (Catalogue#400-ML), IL-1β (Catalogue#401-ML), IL-1Ra (Catalogue#480-RM), IL-2 (Catalogue#402-ML), IL-4 (Catalogue#404-ML), IL-5 (Catalogue#405-ML), IL-8 (Catalogue#208-IL-010), IL-10 (Catalogue#417-ML), IL-12 (Catalogue#419-ML), IL-17A (Catalogue#421-ML), IL-33 (Catalogue#3626-ML), IFNγ (Catalogue#485-ML) (all from R&D Systems), IL-6 (BD Biosciences, Catalogue#554582), TNF (BD Biosciences, Catalogue#554589), GM-CSF (Peprotech, Catalogue#315-03), M-CSF (Sigma-Aldrich, Catalogue#SRP3110), and TGFβ (Miltenyi Biotec, Catalogue#130-095-066), or 10 μg/ml LPS (Sigma-Aldrich, Catalogue#L4391).

For eosinophil-induced differentiation of Siglec-F^{hi} neutrophils, 0.2 million bone marrow neutrophils were co-cultured with 0.1 million lung eosinophils in the culture media described above in 96-well round-bottom plates for 2 days. For each steady-state eosinophil sample, lung eosinophils from four mice were pooled, whereas each asthmatic lung eosinophil sample was isolated from an individual mouse.

For antibody-mediated blocking of Siglec-F^{hi} neutrophil differentiation, asthmatic lung eosinophils were pretreated for 5 min with either a combination of 5 μg/ml anti-IL-4 (BVD4-1D1, BD Biosciences, Catalogue#554387) and 5 μg/ml anti-GM-CSF (MP122E9, R&D Systems, Catalogue#MAB415) or 1 μg/ml anti-PECAM-1 (MEC13.3, Biolegend, Catalogue#102501) and then co-cultured with bone marrow neutrophils. The following isotype control antibodies were used as controls: purified Rat IgG2a, κ (e-bioscience, Catalogue#16-4321-85), and purified Rat IgG2b, κ (BD Biosciences, Catalogue#553985). To achieve physical separation between eosinophils and neutrophils, 0.2 million bone marrow neutrophils were cultured in 24-well flat-bottom plates with 0.4 million asthmatic lung eosinophils placed in 0.4 μm transwell inserts (Corning, Catalogue#CLS3470) for 2 days.

Analysis of eosinophil-neutrophil interaction

Bone marrow neutrophils (0.2 million) were cultured in the presence or absence of asthmatic lung eosinophils (0.1 million) in a 96-well flat bottom plate for 2 days, and cells were imaged using a Nikon ECLIPSE Ts2R microscope (Japan). For fluorescence imaging, bone marrow neutrophils labeled with carboxyfluorescein succinimidyl ester (Thermo Fisher Scientific, Catalogue#C34570) and asthmatic lung eosinophils (0.1 million each) were co-cultured in a 96-well round bottom plate for 4 h. Without any resuspension, cells were carefully transferred into the cytofunnel and attached to a slide glass using Cytospin 4 (Thermo Fisher Scientific). After overnight drying, the cells were fixed with 4% paraformaldehyde, permeabilized with 0.3% Triton X-100 in PBS, and stained with an anti-CD63-APC antibody (NVG-2, Biolegend, Catalogue#143905). Fluorescence images were taken using a Nikon A1 HD25 confocal microscope.

Neutrophil transwell migration assay

Bone marrow neutrophils were labeled with 5 μM CellTrace Violet (CTV, Invitrogen, Catalogue#C34557) at 37 °C for 20 min. CTV-labeled neutrophils (0.1 or 0.2 million) and asthmatic lung eosinophils (0.7 million) were placed in a 3 μm transwell insert (Corning, Catalogue#3385) and the bottom 96-well plate, respectively, and cultured for 24 h. The cells in the bottom plate were resuspended to dissociate the aggregated cells, and CTV-labeled neutrophils were imaged using a Nikon ECLIPSE Ts2R fluorescence microscope.

In vitro Th17 differentiation

To determine the ability of neutrophils to induce Th17 differentiation, Siglec-F^{hi} and Siglec-F^{lo} neutrophils were prepared by culturing bone marrow neutrophils for 2 days in the presence or absence of 10 ng/ml GM-CSF (Peprotech, Catalogue#315-03) and 10 ng/ml IL-4 (R&D Systems, Catalogue#404-ML), respectively. Following differentiation, neutrophils were washed to remove residual IL-4 and GM-CSF, and live cell numbers were recounted before co-culture with naïve CD4 T cells. To prepare naïve CD4 T cells, spleens and peripheral lymph nodes were ground through 100 μm strainers using the piston of 1 ml syringes. After lysing red blood cells with ACK lysis buffer, naïve CD4 T cells were isolated by negative selection with biotin-conjugated antibodies listed in Supplementary Table 2 by using EasySep Mouse Streptavidin RapidSpheres isolation kit (STEMCELL Technologies). Naïve CD4 T cells (0.1 million) were co-cultured with Siglec-F^{hi} or Siglec-F^{lo} neutrophils (0.05 million) in the presence of 5 ng/ml TGFβ (Miltenyi Biotec, Catalogue#130-095-066), 2 ng/ml IL-6 (BD Biosciences, Catalogue#554582), 5 μg/ml anti-IL-4 (BVD4-1D1, BD Biosciences, Catalogue#554387), 2.5 μg/ml anti-IL-2 (S4B6, BD Biosciences, Catalogue#554375), 5 μg/ml anti-IFNγ (R4-6A2, Invitrogen, Catalogue#14-7312-85) in a 96-well flat bottom plate pre-coated with 2.5 μg/ml anti-CD3 (145-2C11, BD Biosciences, Catalogue#553057) and 1 μg/ml anti-CD28 (37.51, BD Biosciences, Catalogue#553294). After 3 days, the frequencies of RORγt or IL-17A-expressing CD4 T cells were analyzed by flow cytometry.

To assess the ability of eosinophils to induce Th17 differentiation, naïve CD4 T cells (0.1 million) were cultured as described above, except that neutrophils were replaced with asthmatic lung eosinophils (0.1 million), and IL-6 was supplied at 20 ng/ml under Th17 differentiation conditions. To assess whether eosinophils indirectly influence Th17 differentiation via dendritic cells, splenic dendritic cells were added to the naïve CD4 T cell-eosinophil co-culture. To prepare the splenic dendritic cells, spleens were chopped into 1 mm^3 fragments and digested with 400 MandlU/ml Collagenase D and 10 μg/ml DNase I in RPMI1640 media containing 3% FBS (Atlas biologicals), 20 mM HEPES, 1 mM non-essential amino acids, 100 U/ml penicillin, 100 μg/ml streptomycin, and 1 mM sodium pyruvate at 37 °C for 30 min with stirring. The cells were centrifuged over 17.5 % Accudenz solution at 805 × *g* for 20 min at room temperature, and the cells at the interface were collected. The dendritic cells were further stained with fluorescent dye-labeled antibodies and purified using BD Biosciences Aria Fusion cell sorter to a purity of over 95%.

Cytokine and chemokine ELISA

To measure cytokine production from T cells in the lung, total asthmatic lung cells (0.5 million) were cultured in flat-bottom 96-well plates coated with 1 μg/ml of anti-CD3 (145-2C11, BD Biosciences, Catalogue#553057) and 1 μg/ml anti-CD28 (37.51, BD Biosciences, Catalogue#553294) for 3 days, and the culture supernatants were collected. To measure neutrophil cytokine production, bone marrow neutrophils (0.3 million) were cultured in the presence of 10 ng/ml IL-4 (R&D Systems, Catalogue#404-ML) or 10 ng/ml GM-CSF (Peprotech, Catalogue#315-03) in 96-well round-bottom plates for 2 days, and the culture supernatants were collected. On the second day of the culture, neutrophils were either stimulated or not with 100 nM PMA (Sigma-Aldrich, Catalogue#79346) and 1 μg/ml ionomycin (Sigma-Aldrich, Catalogue#I9657). To assess cytokine production by asthmatic lung neutrophils, Siglec-F^{lo} and Siglec-F^{hi} neutrophils were sorted from asthmatic lungs based on Siglec-F expression, and eighty thousand cells were cultured in 96-well round-bottom plates for 24 hours without stimulation. To measure cytokine production by asthmatic lung eosinophils, sorted cells (0.5 million) were cultured in 96-well round-bottom plates for 24 hours either without stimulation (for CCL6 and CCL24) or in the presence of 100 nM PMA and 1 μg/ml ionomycin (for CXCL2). To measure cytokine production by bone marrow-derived eosinophils (BMDEs), 0.3 million cells were cultured in 96-well round-bottom plates for 24 hours with stimulation by 10 ng/ml IL-33 (R&D Systems, Catalogue#3626-ML). Antibodies and kits for cytokine ELISA were listed in Supplementary Table 3. Half-Area 96-well microplates (Corning, Catalogue#3690) were coated with 2 μg/ml capture antibodies in PBS at 4 °C overnight and blocked with blocking buffer containing 2% BSA fraction V (Roche, Catalogue#10735108001) in PBS-T (0.05% Tween-20 (Daejung, Catalogue#8571-1405) in PBS) for 1 h at room temperature. Subsequently, samples were added and incubated for 1 h. Thereafter, 1 μg/ml biotin-conjugated antibodies were added for 45 min, followed by treatment with 50 ng/ml streptavidin-horseradish peroxidase (R&D Systems, Catalogue#DY998) for 20 min. Between each step, plates were washed at least 3 times with PBS-T. To develop the reaction, 50 μl of tetramethylbenzidine solution (Surmodics, USA, Catalogue#TMBW) was added, and the reaction was stopped by adding 50 μl of 0.5 M H_2SO_4 (Daejung, Catalogue#7683-4100). Absorbance at O.D.450 nm was read using SpectraMax M2 Microplate Reader (Molecular Devices, USA).

Preparation of bone marrow-derived eosinophils

Bone marrow-derived eosinophils (BMDEs) were differentiated by following the previously described protocol[75]. In brief, bone marrow cells (3 ×106/ml) were differentiated with 100 ng/ml SCF (Peprotech, Catalogue#250-03), and 100 ng/ml FLT3 ligand (R&D Systems, Catalogue#427-FL-025/CF) in RPMI1640 media containing 20 % FBS (Hyclone, Catalogue#SH30919.03), 1 mM non-essential amino acids, 25 mM HEPES, 100 U/ml Penicillin, 100 μg/ml streptomycin, 1 mM sodium pyruvate, 50 μM β-mercaptoethanol, and 2 mM L-glutamine in 6-well plates for 4 days. The medium was then changed to new culture medium containing 10 ng/ml IL-5 (R&D Systems, Catalogue#405-ML). On days 8 and 11, the medium was changed again with new IL-5-containing medium, and the cell number was adjusted to 1 × 106/ml. On day 14, ELISA, Ca^{2+} flux assay, and RNA extraction were performed.

Ca^{2+} flux assay

Cells were loaded with 2 μg/ml Fluo-3 AM (Thermo Fisher Scientific, Catalogue#F23915) and 5 μg/ml Fura Red AM (Thermo Fisher Scientific, Catalogue#F3021) in RPMI1640 medium containing 2% FBS, 25 mM HEPES, 2.5 mM probenecid (Sigma-Aldrich, Catalogue#P8761), and 0.02% pluronic F-127 (Sigma-Aldrich, Catalogue#P2443) at 37 °C for 20 min. After washing, the cells were analyzed using a flow cytometer (LSR Fortessa X-20, BD Biosciences). Basal fluorescence was recorded for 30 seconds, and changes in the fluorescence were recorded for an additional 3 min after stimulating the cells with 10 mM acetate.

RNA extraction

Asthmatic lung eosinophils, BMDEs, and bone marrow neutrophils were lysed in Qiazol (QIAzen, Germany, Catalogue#79306), and chloroform (Daejung, Catalogue#2548-4400) was added in a 5:1 ratio. After centrifugation, the clear upper phase was collected, and RNA was precipitated by adding the same volume of 100% isopropanol (Merck, Catalogue#1.09634.2511) and 20 μg glycogen (Sigma-Aldrich, Catalogue#G1767). After centrifugation, the pellet was washed with 75% ethyl alcohol (Merck, Catalogue#1.00983.2511) diluted in DEPC water (Biosesang, South Korea, Catalogue#WR2004-050-00) and air-dried. RNA was solubilized in nuclease-free water (Invitrogen, Catalogue#AM9930).

Quantitative PCR

RNAs were reverse-transcribed to cDNA using GoScript 5X reaction buffer (Catalogue#A500C), reverse transcriptase (Catalogue#A501C), ribonuclease inhibitor (Catalogue#N251B), dNTP (Catalogue#U151B), MgCl2 (Catalogue#A351H), and oligo(dT)15 primer (Catalogue#C110A) (all from Promega). Using cDNAs as templates, qPCR analysis of genes of interest was performed with SYBR Green Realtime PCR Master Mix

(TOYOBO, Japan, Catalogue#QPK-201) and CFX Connect Real-Time System (Bio-Rad). Gene expression levels were calculated based on the comparative Cq method and normalized to *Hprt* gene expression. Primers are described in Supplementary Table 4.

Bulk-RNA sequencing

The integrity of asthmatic lung eosinophil RNA was measured using a Bioanalyzer 2100 (Agilent Technologies, USA). Ribosomal RNAs were removed using NEBNext rRNA Depletion Kit v2 (USA, Catalogue#E7405L), and the cDNA library was synthesized using NEBNext Ultra II Directional RNA Library Prep kit (Catalogue#E7765S) according to the manufacturer's protocols. Sequencing was conducted on an Illumina HiSeq2500 with paired-ended reads of 100 base pairs by Macrogen (South Korea). Fastq files were trimmed with the package Fastp and aligned to the mm10 mouse reference genome sequences with STAR. Transcript per million (TPM) was calculated from the counts obtained with FeatureCounts, and differentially expressed genes (DEGs) were acquired from the raw counts with DESeq2 by using a *p*-value below 0.05. All processes were conducted through Galaxy (https://usegalaxy.org/). Additional pathway analysis was performed using pathfindR and Clusterprofiler in R v.4.3.1. Publicly available bulk-RNA sequencing data for eosinophils from mouse spleen[26], peritoneal cavity[26], lung[24], colon[25], skin[14], blood[14], bone marrow[14], BMDE[27], and human peripheral blood[28] were analyzed with the same processes (Supplementary Table 5).

Single-cell RNA sequencing

Asthmatic lung cells from $Epx^{Cre/+}$ and $Epx^{Cre/+}Gpr43^{fl/fl}$ mice were isolated from 3 mice per genotype, pooled, and stained with Ghost dye Red780 (TONBO, Catalogue#13-0865-T100). Live cells, excluding FSC^{hi} SSC^{hi} cells, were sorted and suspended in PBS containing 0.04% BSA. The total of 28,320 and 25,620 cells from $Epx^{Cre/+}$ and $Epx^{Cre/+}Gpr43^{fl/fl}$ mice, respectively, were loaded onto Chromium-controller (10X Genomics), and scRNA-seq libraries were generated by using the Chromium Next GEM Single Cell 3′ Reagent Kits v 3.1 (10X Genomics, Catalogue#PN-1000268) according to the manufacturer's protocol at the KAIST NGS core facility. Sequencing was performed on a HiSeqX platform by Macrogen (South Korea).

Raw sequencing files were initially processed with the Cell Ranger (v.4.0.0) pipeline, using the mm10 reference, and downstream analysis was conducted based on the Scanpy (v.1.8.2) pipeline. Low-quality cells meeting any one of the following criteria were excluded in the downstream analysis: (1) UMI gene count <1000, (2) number of genes detected <500, (3) number of genes detected > 7000, (4) fraction of mitochondrial genes > 10%, and (5) predicted doublets identified with the Scrublet (v.0.2.2) package. Raw counts were normalized in each cell (100,000 counts per cell) and log-transformed (log1p). Highly variable genes ($n = 2,418$) were selected by using the highly_variable_genes function in the Scanpy package. Principal component analysis (PCA) was conducted (n_PCs = 50) on the scaled expression values of the highly variable genes. Neighborhood graphs of the cells were constructed (n_neighbors = 15) based on PC coordinates, and the Uniform Manifold Approximation and Projection (UMAP) embedding of the cells was calculated. After the preprocessing steps, 3,989 cells from the $Epx^{Cre/+}$ sample and 4,871 cells from the $Epx^{Cre/+}Gpr43^{fl/fl}$ sample were retrieved and analyzed. Wilcoxon rank-sum test was used for the DEG analysis, and *p*-values were adjusted with the Benjamini-Hochberg method.

For gene set enrichment analysis (GSEA) of DEGs between Siglec-F^{lo} and Siglec-F^{hi} neutrophils, a pre-ranked gene set was created by listing 3515 DEGs with an adjusted *p*-value of less than 0.05, ranked by test statistics score using GSEApy v.1.1.3. Normalized enrichment scores (NES) and false discovery rates (FDR) were obtained by using following parameters: (1) number of permutations = 1000, (2) permutation type: gene set, and (3) weighted enrichment statistics. Significant gene sets were those with an FDR < 0.25 and *p*-value < 0.05. Gene sets for the analysis were obtained from the Kyoto Encyclopedia of Genes and Genomes (KEGG) and Gene Ontology (GO) databases. To compare the Siglec-F^{hi} neutrophils identified in our HDM-induced asthma model to those in other disease models using publicly available transcriptomic data[33–35], another pre-ranked gene set was generated by ranking the same 3515 DEGs according to LogFC values. Gene lists for the Siglec-F^{hi} neutrophil signature genes in the other disease models were generated, using the top 350 DEGs between Siglec-F^{lo} and Siglec-F^{hi} neutrophils in each disease model, and ranked based on LogFC values.

Analysis of publicly available scRNA-seq data was performed using Seurat v4.1.3. Matrix (mtx) files for esophagus and duodenum samples from 10 eosinophilic esophagitis patients were downloaded (GSE175930)[29] together with feature and cell information files (Supplementary Table 5), and Seuratobject was created. Low-quality cells meeting any one of the following criteria were excluded in the downstream analysis: (1) min.cells <3, (2) min.features <200, (3) number of genes detected <200, (4) number of genes detected > 6000, and (5) fraction of mitochondrial genes > 20%. Seuratobjects were normalized, and highly variable genes were found by using the vst selection method. Each esophagus and duodenum sample was integrated separately (n_dimension = 50), and PCA was conducted (n_PC = 30). Neighborhood graphs of the cells were constructed (n_dimension = 30), UMAP was created, and the cells were clustered (esophagus: resolution = 0.3; duodenum: resolution = 0.1). Each cluster was manually annotated using known marker genes.

Statistical analysis

All data points represent biological replicates unless otherwise noted. Specifically, Fig. 4a–c show experimental replicates, and Fig. 6g and Supplementary Fig. 9e show technical replicates. For all technical replicate experiments, results were confirmed in at least three independent experiments. For comparisons between two groups, either a paired or unpaired two-tailed Student's t-test was performed, depending on sample matching. One-way ANOVA with Tukey's multiple comparisons test was used to compare the means of three or more groups with a single independent variable. To evaluate the effects of two independent variables and their interaction, two-way ANOVA with Tukey's multiple comparisons test was conducted. Statistical analyses were performed with GraphPad Prism v8.4.2.

Reporting summary

Further information on the research design is available in the Nature Research Reporting Summary linked to this article.

Reporting summary

Further information on research design is available in the Nature Portfolio Reporting Summary linked to this article.

Data availability

The raw and processed bulk RNA-seq data (expression matrix) from asthmatic lung eosinophils have been deposited in the Gene Expression Omnibus under accession code GSE271832. In addition, a filtered expression matrix (genes with an average TPM ≥ 5 across samples) is also provided in Supplementary Data 1. The raw and processed single-cell RNA-seq data (expression matrix and associated metadata) from whole asthmatic lung cells are available under accession code GSE271835. Additional information on previously published datasets used in this study is provided in Supplementary Table 5. All data are included in this article, the Supplementary Information, and the Source Data file. Raw data files for flow cytometry analysis are available from the authors upon reasonable requests. Source data are provided with this paper.

References

1. Rothenberg, M. E. & Hogan, S. P. The eosinophil. *Annu Rev. Immunol.* **24**, 147–174 (2006).
2. Weller, P. F. & Spencer, L. A. Functions of tissue-resident eosinophils. *Nat. Rev. Immunol.* **17**, 746–760 (2017).
3. Arnold, I. C. & Munitz, A. Spatial adaptation of eosinophils and their emerging roles in homeostasis, infection and disease. *Nat. Rev. Immunol.* https://doi.org/10.1038/s41577-024-01048-y (2024).
4. Lee, J. J., Jacobsen, E. A., McGarry, M. P., Schleimer, R. P. & Lee, N. A. Eosinophils in health and disease: the LIAR hypothesis. *Clin. Exp. Allergy* **40**, 563–575 (2010).
5. Kanda, A. et al. The multiple functions and subpopulations of eosinophils in tissues under steady-state and pathological conditions. *Allergol. Int* **70**, 9–18 (2021).
6. Wu, D. et al. Eosinophils sustain adipose alternatively activated macrophages associated with glucose homeostasis. *Science* **332**, 243–247 (2011).
7. Arnold, I. C. et al. Eosinophils suppress Th1 responses and restrict bacterially induced gastrointestinal inflammation. *J. Exp. Med* **215**, 2055–2072 (2018).
8. Sugawara, R. et al. Small intestinal eosinophils regulate Th17 cells by producing IL-1 receptor antagonist. *J. Exp. Med* **213**, 555–567 (2016).
9. Mesnil, C. et al. Lung-resident eosinophils represent a distinct regulatory eosinophil subset. *J. Clin. Invest* **126**, 3279–3295 (2016).
10. Dougan, M., Dranoff, G. & Dougan, S. K. GM-CSF, IL-3, and IL-5 Family of cytokines: Regulators of inflammation. *Immunity* **50**, 796–811 (2019).
11. Diny, N. L. et al. The aryl hydrocarbon receptor contributes to tissue adaptation of intestinal eosinophils in mice. *J. Exp. Med.* **219**, https://doi.org/10.1084/jem.20210970 (2022).
12. Wang, W. L. et al. The aryl hydrocarbon receptor instructs the immunomodulatory profile of a subset of Clec4a4(+) eosinophils unique to the small intestine. *Proc. Natl Acad. Sci. USA* **119**, e2204557119 (2022).
13. Vassily, I. K., Korn, L. L. & Medzhitov, R. Nutrient-derived signals regulate eosinophil adaptation to the small intestine. *Proc. Natl Acad. Sci. USA* **121**, e2316446121 (2024).
14. Li, Y. et al. Neuromedin U programs eosinophils to promote mucosal immunity of the small intestine. *Science* **381**, 1189–1196 (2023).
15. Koh, A., De Vadder, F., Kovatcheva-Datchary, P. & Backhed, F. From Dietary Fiber to Host Physiology: Short-Chain Fatty Acids as Key Bacterial Metabolites. *Cell* **165**, 1332–1345 (2016).
16. Tan, J. K., Macia, L. & Mackay, C. R. Dietary fiber and SCFAs in the regulation of mucosal immunity. *J. Allergy Clin. Immunol.* **151**, 361–370 (2023).
17. Yoon, J. H., Do, J. S., Velankanni, P., Lee, C. G. & Kwon, H. K. Gut microbial metabolites on host immune responses in health and disease. *Immune Netw.* **23**, e6 (2023).
18. Maslowski, K. M. et al. Regulation of inflammatory responses by gut microbiota and chemoattractant receptor GPR43. *Nature* **461**, 1282–1286 (2009).
19. Theiler, A. et al. Butyrate ameliorates allergic airway inflammation by limiting eosinophil trafficking and survival. *J. Allergy Clin. Immunol.* **144**, 764–776 (2019).
20. Tan, J. et al. Dietary fiber and bacterial scfa enhance oral tolerance and protect against food allergy through diverse cellular pathways. *Cell Rep.* **15**, 2809–2824 (2016).
21. Mann, E. R., Lam, Y. K. & Uhlig, H. H. Short-chain fatty acids: linking diet, the microbiome and immunity. *Nat. Rev. Immunol.* 10.1038/s41577-024-01014-8 (2024).
22. Wu, W. et al. Microbiota metabolite short-chain fatty acid acetate promotes intestinal IgA response to microbiota which is mediated by GPR43. *Mucosal Immunol.* **10**, 946–956 (2017).
23. Chun, E. et al. Metabolite-sensing receptor ffar2 regulates colonic group 3 innate lymphoid cells and gut immunity. *Immunity* **51**, 871–884.e876 (2019).
24. Motomura, Y. et al. Basophil-derived interleukin-4 controls the function of natural helper cells, a member of ILC2s, in lung inflammation. *Immunity* **40**, 758–771 (2014).
25. Grace, J. O. et al. Reuse of public, genome-wide, murine eosinophil expression data for hypotheses development. *J. Leukoc. Biol.* **104**, 185–193 (2018).
26. Yoshida, H. et al. The cis-regulatory atlas of the mouse immune system. *Cell* **176**, 897–912.e820 (2019).
27. Arnold, I. C. et al. The GM-CSF-IRF5 signaling axis in eosinophils promotes antitumor immunity through activation of type 1 T cell responses. *J. Exp. Med.* **217**, https://doi.org/10.1084/jem.20190706 (2020).
28. Van Hulst, G. et al. Anti-IL5 mepolizumab minimally influences residual blood eosinophils in severe asthma. *Eur. Respi.r J.* **59**, https://doi.org/10.1183/13993003.00935-2021 (2022).
29. Morgan, D. M. et al. Clonally expanded, GPR15-expressing pathogenic effector T(H)2 cells are associated with eosinophilic esophagitis. *Sci. Immunol.* **6**, https://doi.org/10.1126/sciimmunol.abi5586 (2021).
30. Wang, L. et al. Single-cell transcriptomic analysis reveals the immune landscape of lung in steroid-resistant asthma exacerbation. *Proc. Natl Acad. Sci. USA* **118**, https://doi.org/10.1073/pnas.2005590118 (2021).
31. Travaglini, K. J. et al. A molecular cell atlas of the human lung from single-cell RNA sequencing. *Nature* **587**, 619–625 (2020).
32. Borrelli, C., Gurtner, A., Arnold, I. C. & Moor, A. E. Stress-free single-cell transcriptomic profiling and functional genomics of murine eosinophils. *Nat. Protoc.* **19**, 1679–1709 (2024).
33. Engblom, C. et al. Osteoblasts remotely supply lung tumors with cancer-promoting SiglecF(high) neutrophils. *Science* **358**, https://doi.org/10.1126/science.aal5081 (2017).
34. Calcagno, D. M. et al. SiglecF(HI) Marks late-stage neutrophils of the infarcted heart: A single-cell transcriptomic analysis of neutrophil diversification. *J. Am. Heart Assoc.* **10**, e019019 (2021).
35. Shin, J. W. et al. A unique population of neutrophils generated by air pollutant-induced lung damage exacerbates airway inflammation. *J. Allergy Clin. Immunol.* **149**, 1253–1269.e1258 (2022).
36. Borkner, L., Curham, L. M., Wilk, M. M., Moran, B. & Mills, K. H. G. IL-17 mediates protective immunity against nasal infection with Bordetella pertussis by mobilizing neutrophils, especially Siglec-F(+) neutrophils. *Mucosal Immunol.* **14**, 1183–1202 (2021).
37. Muniz-Junqueira, M. I., Barbosa-Marques, S. M. & Junqueira, L. F. Jr. Morphological changes in eosinophils are reliable markers of the severity of an acute asthma exacerbation in children. *Allergy* **68**, 911–920 (2013).
38. Lionakis, M. S. et al. Chemokine receptor Ccr1 drives neutrophil-mediated kidney immunopathology and mortality in invasive candidiasis. *PLoS Pathog.* **8**, e1002865 (2012).
39. Grigolato, F., Egholm, C., Impellizzieri, D., Arosio, P. & Boyman, O. Establishment of a scalable microfluidic assay for characterization of population-based neutrophil chemotaxis. *Allergy* **75**, 1382–1393 (2020).
40. Muller, W. A., Weigl, S. A., Deng, X. & Phillips, D. M. PECAM-1 is required for transendothelial migration of leukocytes. *J. Exp. Med* **178**, 449–460 (1993).
41. Privratsky, J. R., Newman, D. K. & Newman, P. J. PECAM-1: conflicts of interest in inflammation. *Life Sci.* **87**, 69–82 (2010).
42. Spencer, L. A. & Weller, P. F. Eosinophils and Th2 immunity: contemporary insights. *Immunol. Cell Biol.* **88**, 250–256 (2010).
43. Akuthota, P., Wang, H. & Weller, P. F. Eosinophils as antigen-presenting cells in allergic upper airway disease. *Curr. Opin. Allergy Clin. Immunol.* **10**, 14–19 (2010).

44. Ambhore, N. S., Kalidhindi, R. S. R., Loganathan, J. & Sathish, V. Role of differential estrogen receptor activation in airway hyperreactivity and remodeling in a murine model of asthma. *Am. J. Respir. Cell Mol. Biol.* **61**, 469–480 (2019).
45. Shah, R. & Newcomb, D. C. Sex bias in asthma prevalence and pathogenesis. *Front Immunol.* **9**, 2997 (2018).
46. Chiarella, S. E. et al. Sex differences in a murine model of asthma are time and tissue-compartment-dependent. *PLoS One* **18**, e0271281 (2023).
47. Zhu, C. et al. Homeostatic and early-recruited CD101(-) eosinophils suppress endotoxin-induced acute lung injury. *Eur. Respir. J.* **56**, https://doi.org/10.1183/13993003.02354-2019 (2020).
48. Jacobsen, E. A. et al. Eosinophil activities modulate the immune/inflammatory character of allergic respiratory responses in mice. *Allergy* **69**, 315–327 (2014).
49. Hammad, H. & Lambrecht, B. N. The basic immunology of asthma. *Cell* **184**, 1469–1485 (2021).
50. Davoine, F. & Lacy, P. Eosinophil cytokines, chemokines, and growth factors: emerging roles in immunity. *Front Immunol.* **5**, 570 (2014).
51. Ryu, S. et al. Siglec-F-expressing neutrophils are essential for creating a profibrotic microenvironment in renal fibrosis. *J. Clin. Invest.* **132**, https://doi.org/10.1172/JCI156876 (2022).
52. Marelli-Berg, F. M., Clement, M., Mauro, C. & Caligiuri, G. An immunologist's guide to CD31 function in T-cells. *J. Cell Sci.* **126**, 2343–2352 (2013).
53. Lee, Y. et al. Induction and molecular signature of pathogenic TH17 cells. *Nat. Immunol.* **13**, 991–999 (2012).
54. Chung, Y. et al. Critical regulation of early Th17 cell differentiation by interleukin-1 signaling. *Immunity* **30**, 576–587 (2009).
55. Fan, X., Shu, P., Wang, Y., Ji, N. & Zhang, D. Interactions between neutrophils and T-helper 17 cells. *Front Immunol.* **14**, 1279837 (2023).
56. Shrestha, S. & Hong, C. W. Extracellular mechanisms of neutrophils in immune cell crosstalk. *Immune Netw.* **23**, e38 (2023).
57. Radzikowska, U. & Golebski, K. Sex hormones and asthma: The role of estrogen in asthma development and severity. *Allergy* **78**, 620–622 (2023).
58. Trivedi, S. et al. Progesterone amplifies allergic inflammation and airway pathology in association with higher lung ILC2 responses. *Am. J. Physiol. Lung Cell Mol. Physiol.* **327**, L65–L78 (2024).
59. Laffont, S., Blanquart, E. & Guery, J. C. Sex differences in asthma: A key role of androgen-signaling in group 2 innate lymphoid cells. *Front Immunol.* **8**, 1069 (2017).
60. Massaro, D. & Massaro, G. D. Estrogen receptor regulation of pulmonary alveolar dimensions: alveolar sexual dimorphism in mice. *Am. J. Physiol. Lung Cell Mol. Physiol.* **290**, L866–L870 (2006).
61. Ekpruke, C. D., Alford, R., Parker, E. & Silveyra, P. Gonadal sex and chromosome complement influence the gut microbiome in a mouse model of allergic airway inflammation. *Physiol. Genomics* **56**, 417–425 (2024).
62. Gao, A. et al. Sexual dimorphism in glucose metabolism is shaped by androgen-driven gut microbiome. *Nat. Commun.* **12**, 7080 (2021).
63. Markle, J. G. et al. Sex differences in the gut microbiome drive hormone-dependent regulation of autoimmunity. *Science* **339**, 1084–1088 (2013).
64. LaBouyer, M. et al. Higher total faecal short-chain fatty acid concentrations correlate with increasing proportions of butyrate and decreasing proportions of branched-chain fatty acids across multiple human studies. *Gut Microbiome (Camb.)* **3**, e2 (2022).
65. Sun, Q. H. et al. Sex-based differences in fecal short-chain fatty acid and gut microbiota in irritable bowel syndrome patients. *J. Dig. Dis.* **22**, 246–255 (2021).
66. Stapleton, S., Welch, G., DiBerardo, L. & Freeman, L. R. Sex differences in a mouse model of diet-induced obesity: the role of the gut microbiome. *Biol. Sex. Differ.* **15**, 5 (2024).
67. Lambrecht, B. N. & Hammad, H. The immunology of asthma. *Nat. Immunol.* **16**, 45–56 (2015).
68. Carr, T. F., Zeki, A. A. & Kraft, M. Eosinophilic and noneosinophilic asthma. *Am. J. Respir. Crit. Care Med* **197**, 22–37 (2018).
69. Irvin, C. et al. Increased frequency of dual-positive TH2/TH17 cells in bronchoalveolar lavage fluid characterizes a population of patients with severe asthma. *J. Allergy Clin. Immunol.* **134**, 1175–1186.e1177 (2014).
70. Liu, W. et al. Mechanism of T(H)2/T(H)17-predominant and neutrophilic T(H)2/T(H)17-low subtypes of asthma. *J. Allergy Clin. Immunol.* **139**, 1548–1558.e1544 (2017).
71. Choy, D. F. et al. TH2 and TH17 inflammatory pathways are reciprocally regulated in asthma. *Sci. Transl. Med* **7**, 301ra129 (2015).
72. Doyle, A. D. et al. Homologous recombination into the eosinophil peroxidase locus generates a strain of mice expressing Cre recombinase exclusively in eosinophils. *J. Leukoc. Biol.* **94**, 17–24 (2013).
73. Srinivas, S. et al. Cre reporter strains produced by targeted insertion of EYFP and ECFP into the ROSA26 locus. *BMC Dev. Biol.* **1**, 4 (2001).
74. Kimura, I. et al. The gut microbiota suppresses insulin-mediated fat accumulation via the short-chain fatty acid receptor GPR43. *Nat. Commun.* **4**, 1829 (2013).
75. Dyer, K. D. et al. Functionally competent eosinophils differentiated ex vivo in high purity from normal mouse bone marrow. *J. Immunol.* **181**, 4004–4009 (2008).

Acknowledgements

The authors thank the scientific contributions and technical assistance by Dr. Yongsuk Hur at the EM & Histology Core Facility and Ms. Jiye Kim at the NGS Core Facility in the BioMedical Research Center, KAIST. This study was supported by grants from Korea Advanced Institute of Science and Technology and the National Research Foundation of Korea (2022R1A6A3A1306363412 to JY; RS-2024-00439160 and RS-2025-02232977 to YMK).

Author contributions

Y.M.K. and J.Y. conceived the project and wrote the manuscript with comments from all authors. J.Y. performed the overall experiments and sequencing data analysis. S.K. and J.E.P. conducted single-cell RNA sequencing data analysis. H.S.S. performed confocal microscopy. J.K. and W.S. provided experimental support. I.K. provided critical resources. H.Y.K. offered technical advices on in vivo experiments and critical input on data interpretation. Y.M.K. supervised the study.

Competing interests

The authors declare no competing interests.

Additional information

Supplementary information The online version contains supplementary material available at https://doi.org/10.1038/s41467-025-65573-7.

Correspondence and requests for materials should be addressed to You-Me Kim.

Peer review information *Nature Communications* thanks Francis Luscinskas, and the other, anonymous, reviewer(s) for their contribution to the peer review of this work. A peer review file is available.